

1987

An analysis of trailing edge flows /

Utham Sobrun
Lehigh University

Follow this and additional works at: <https://preserve.lehigh.edu/etd>



Part of the [Mechanical Engineering Commons](#)

Recommended Citation

Sobrun, Utham, "An analysis of trailing edge flows /" (1987). *Theses and Dissertations*. 4784.
<https://preserve.lehigh.edu/etd/4784>

This Thesis is brought to you for free and open access by Lehigh Preserve. It has been accepted for inclusion in Theses and Dissertations by an authorized administrator of Lehigh Preserve. For more information, please contact preserve@lehigh.edu.

AN ANALYSIS OF TRAILING EDGE FLOWS

by

Utham Sobrun

A Thesis

Presented to the Graduate Committee

of Lehigh University

in Candidacy for the Degree of

Master of Science

in

Division of Engineering Mathematics

Department of Mechanical Engineering and Mechanics

Lehigh University

1987

This thesis is accepted and approved in
partial fulfillment of the requirements
for the degree of Master of Science.

May 6, 1987

(date)

JDA Walker

Professor in Charge

F. Erdogan

Chairman of Mechanical

Engineering and Mechanics

TABLE OF CONTENTS

Title Page	i
Certificate of Approval	ii
List of Figures	iv
Nomenclature	vi
Abstract	1
1 Introduction	2
2 Statement of the Problem	4
3 Mathematical Formulation	7
4 Open Wake Solution	19
4.1 Solution Technique	19
4.2 Numerical Scheme and Procedure	22
5 Results and Discussion	26
Figures	28
List of References	46
Biography	47

LIST OF FIGURES

Figure 2.1	Coordinate system for separation at a square trailing edge.	6
Figure 3.1	Hodograph mapping of (x,y) plane onto (ϕ,ψ) plane.	13
Figure 5.1a	Wake profiles for $\theta = 0.5$.	28
Figure 5.1b	Wake profiles in the physical space for $\theta = 0.5$.	29
Figure 5.2a	Wake profile for $\theta = 0.5$; Failure.	30
Figure 5.2b	Wake profile in the physical space for $\theta = 0.5$; Failure.	31
Figure 5.3a	Wake profile for $\theta = 0.5$; Failure mode.	32
Figure 5.3b	Wake profile in the physical space for $\theta = 0.5$; Failure mode.	33
Figure 5.4a	Wake profile for $\theta = 0.7$.	34
Figure 5.4b	Wake profile in the physical space for $\theta = 0.7$.	35
Figure 5.5a	Wake profile for $\theta = 0.7$; Failure.	36
Figure 5.5b	Wake profile in the physical space for $\theta = 0.7$; Failure.	37
Figure 5.6a	Wake profile for $\theta = 0.7$; Failure mode.	38
Figure 5.6b	Wake profile in the physical space for $\theta = 0.7$; Failure mode.	39
Figure 5.7a	Wake profile for $\theta = 0.9$.	40

Figure 5.7b	Wake profile in the physical space for $\theta = 0.9$.	41
Figure 5.8a	Wake profile for $\theta = 0.9$; Failure.	42
Figure 5.8b	Wake profile in the physical space for $\theta = 0.9$; Failure.	43
Figure 5.9a	Wake profile for $\theta = 0.9$; Failure mode.	44
Figure 5.9b	Wake profile in the physical space for $\theta = 0.9$; Failure mode.	45

NOMENCLATURE

- A Dimensionless parameter associated with the vorticity in the wake region.
- c_i Bernoulli constant in the wake region.
- c_o Bernoulli constant outside the wake region.
- d Half thickness of flat plate.
- f Wake profile function in the physical space.
- F Wake profile function in the hodograph space.
- P_i Dimensionless pressure inside wake boundary.
- P_o Dimensionless pressure outside wake boundary.
- Re Reynolds number.
- u Dimensionless streamwise velocity.
- U_∞ Dimensionless mainstream streamwise velocity.
- U_T Representative velocity in the wake region.
- v Dimensionless normal velocity.
- x Dimensionless streamwise coordinate.
- \bar{x} Perturbation function in the hodograph plane; Equation (3.20).
- x^* Streamwise coordinate.
- \bar{y} Perturbation function in the hodograph plane; Equation (3.20).
- y Dimensionless normal coordinate.
- y^* Normal coordinate.

- l Length of wake in the physical space.
- θ Dimensionless parameter associated with the constant vorticity wake region.
- λ Dimensionless wake length in the physical space.
- ρ Density of fluid.
- ϕ Potential function.
- ϕ_λ Dimensionless wake length in the hodograph space.
- ψ Stream function.
- ω Constant vorticity in the wake region.

ABSTRACT

In this study a model for the separated flow field behind a long thick flat body oriented parallel to a uniform flow is investigated. A model problem of flow over a flat plate of finite thickness with a square trailing edge is considered. The flow separates at the trailing edge resulting in a separated wake region which is modelled as a pair of long recirculating eddies of uniform vorticity. The flow field exterior to the separated region is considered to be irrotational and inviscid.

The problem is the determination of the shape of the streamline defining the edge of the separated wake region, for given levels of vorticity within the separated region, as well as the length of the wake.

With the assumptions that the long eddy approximation is valid along the dividing streamline and the tangential velocity is discontinuous across the boundary of the separated region, it is shown that the shape function satisfies a nonlinear integro-differential equation. This equation is solved using an iterative numerical integration scheme. The results are illustrated by a series of plots of the shape function.

Limited success is achieved in the sense that short wakes are observed in contrast to the long eddy assumption and the solutions obtained are only acceptable in a limited parameter range.

1. INTRODUCTION

The flow of a fluid past a rigid body occurs in a wide range of practical applications. For fluids such as water and air which have small kinematic viscosity, the flow Reynolds number is usually very high. The effects of viscosity give rise to thin hydrodynamic boundary layer regions adjacent to the body surface. When the body temperature is different from that of the bulk flow, thermal boundary layers also exist near the body surface.

Convection heat transfer problems occur in many engineering applications such as gas turbines and flow over aircraft wings; hence the ability to determine surface drag and heat transfer rates is necessary in engineering design.

An area of particular interest is the trailing edge of a body. Trailing edge contours may be sharp or blunt. In the case of a thick flat plate with a blunt trailing edge, high Reynolds number flows undergo complex boundary layer separation at the trailing edge, giving rise to a rotational wake flow region behind the body. A prerequisite for addressing the heat transfer problem at the trailing edge is an understanding of the fluid flow field there. Experimental studies by Haji-Haidari and Smith (1984) show that for a long thick flat plate with a trailing edge having the shape of a circular cylinder, the mean flow at the trailing edge appears as a double-eddy separation bubble.

In this study the Prandtl-Batchelor model proposed by Batchelor (1956a, 1956b) is adopted for the time mean separation bubble. For

this model, the separated wake region is considered to be bounded by thin shear layers which become dividing streamlines in the limit $Re \rightarrow \infty$.

Furthermore, flow in the rotational wake region is considered to be effectively inviscid and of constant vorticity.

As a simple model problem, a thick flat plate with a square trailing edge is selected since the location of the separation points at the square corners is known a priori. Furthermore, it is expected (Batchelor, 1981) that the boundary layer separates at the square edge and leaves the edge tangentially to the upstream face.

The main objective of this study is to determine the shape and the extent of the separated wake region.

2. STATEMENT OF THE PROBLEM

A long thick flat plate with a square trailing edge is oriented parallel to a uniform flow. The flow which approaches the trailing edge ultimately evolves into a wake flow. As a simplifying assumption, the flow approaching the trailing edge is assumed to be irrotational and inviscid. The flow separation points for a square geometry are fixed at the corners as indicated in Figure 2.1. The plate is assumed to have a smooth leading edge and the plate thickness, $2d$, is considered small with respect to the length L . The cartesian coordinates x^* and y^* are centered on the trailing edge and the profile of the separated region attached to the trailing edge is given by $y^* = d\tilde{f}(x^*)$ with $\tilde{f}(x^*)$ satisfying

$$\tilde{f}(0) = 1, \quad \tilde{f}(\ell) = 0 ; \quad (2.1)$$

ℓ is the unknown wake length in the x^* direction. It is assumed that the flow leaves the separation point tangentially (Bachelor, 1981) so that

$$\tilde{f}'(0) = 0. \quad (2.2)$$

At large distances from the body the flow is assumed to approach a uniform flow speed U_{∞}^* corresponding to uniform flow far upstream. The flow field outside the separated region is inviscid and irrotational. For the flow in the separated wake region the Prandtl- Batchelor model is adopted. In accordance with this model, the separated wake region is bounded by thin shear layers which become dividing streamlines in the limit $Re \rightarrow \infty$. Furthermore, flow in this region is considered to be effectively inviscid, rotational and of constant vorticity. The is then to determine the length and the shape of the separated wake for a given level of vorticity.

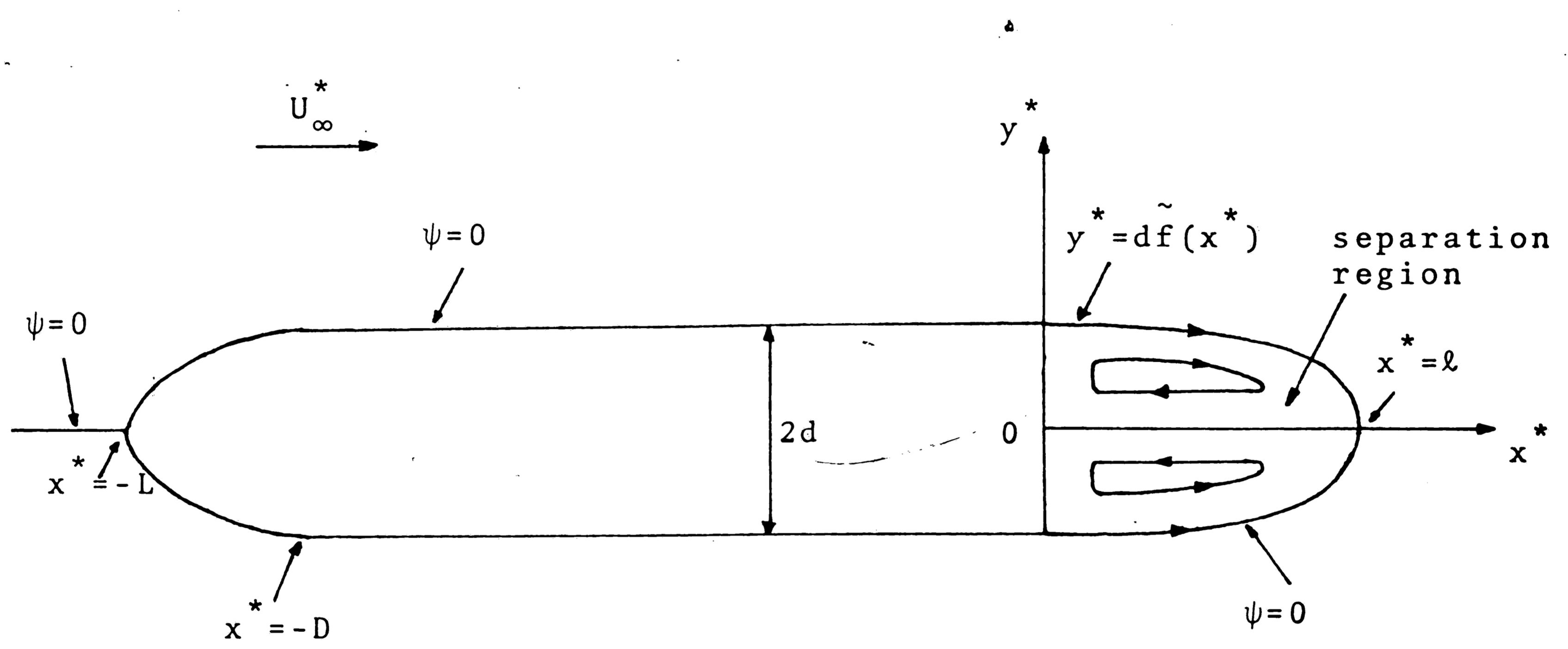


Figure 2.1: Coordinate system for separation at a square trailing edge.

3. MATHEMATICAL FORMULATION.

Introduce the following non-dimensional variables;

$$u = \frac{u^*}{U_\infty^*}, \quad v = \frac{v^*}{U_\infty^*}, \quad x = \frac{x^*}{d}, \quad y = \frac{y^*}{d}. \quad (3.1)$$

Define a velocity potential function ϕ and a stream function ψ by

$$u = \frac{\partial \phi}{\partial x} = \frac{\partial \psi}{\partial y}, \quad v = \frac{\partial \phi}{\partial y} = -\frac{\partial \psi}{\partial x}. \quad (3.2)$$

Since the flow field outside the body is irrotational, ϕ and ψ satisfy the continuity equation

$$\nabla^2 \phi = 0, \quad \nabla^2 \psi = 0, \quad (3.3)$$

where

$$\nabla^2 = \frac{\partial^2}{\partial x^2} + \frac{\partial^2}{\partial y^2} \quad (3.4)$$

is the Laplacian operator in two dimensions and

$$\psi \rightarrow y, \quad \phi \rightarrow x \quad \text{as} \quad x^2 + y^2 \rightarrow \infty. \quad (3.5)$$

The $\psi = 0$ streamline defines the shape of the body and the boundary of the wake region. In the separated wake region the flow is assumed to be inviscid and the vorticity constant (Batchelor; 1956a,1956b) and equal to 2ω . The equation for the stream function is

$$\nabla^2 \psi = \frac{2}{\theta}, \quad (3.6)$$

where the dimensionless constant θ is defined by

$$\theta = \frac{U_{\infty}^*}{\omega d} = \frac{U_{\infty}^*}{U_T}, \quad (3.7)$$

$U_T = \omega d$ is a representative velocity in the wake region.

The basic assumption in the subsequent analysis is that the separated eddy is long in relation to the thickness of the plate, hence,

$$\lambda = \frac{\ell}{d} \gg 1. \quad (3.8)$$

Consequently gradients in the x direction may be neglected with respect to those in the y direction. This is the long eddy approximation. Using this approximation equation (3.6) reduces to

$$\frac{\partial^2 \psi}{\partial y^2} = \frac{2}{\theta}. \quad (3.9)$$

The general solution of equation (3.9) with the conditions $\psi = 0$ on the centerline $y = 0$ and on the wake boundary $y = f(x)$ is

$$\psi = \frac{y}{\theta} [y - f(x)]. \quad (3.10)$$

It follows from equation (3.10) that the velocity components within the wake region are

$$u = \frac{1}{\theta} [2y - f(x)], \quad v = \frac{y}{\theta} f'(x). \quad (3.11)$$

Near the eddy edge, $y \simeq f(x)$ and the velocity components become

$$u = \frac{f(x)}{\theta}, \quad v = \frac{f(x)}{\theta} f'(x). \quad (3.12)$$

The shape function $f(x)$ is to satisfy the boundary conditions

$$f(0) = 1, \quad f(\lambda) = 0. \quad (3.13)$$

Furthermore, it is assumed that the flow leaves the trailing edge tangentially so that

$$f'(0) = 0. \quad (3.14)$$

In the region external to the separated wake, the stream function $\psi(x,y)$ and the potential $\phi(x,y)$ are assumed analytic. Hence for each ψ and ϕ there exists x and y such that

$$x = x(\phi, \psi), \quad y = y(\phi, \psi). \quad (3.15)$$

Under this hodograph transformation, ϕ and ψ become independent variables with respect to x and y . Differentiation of equations (3.15) with respect to x and y yields

$$\begin{aligned} 1 &= \frac{\partial \phi}{\partial x} \frac{\partial x}{\partial \phi} + \frac{\partial \psi}{\partial x} \frac{\partial x}{\partial \psi} = u \frac{\partial x}{\partial \phi} - v \frac{\partial x}{\partial \psi}, \\ 0 &= \frac{\partial \phi}{\partial y} \frac{\partial x}{\partial \phi} + \frac{\partial \psi}{\partial y} \frac{\partial x}{\partial \psi} = v \frac{\partial x}{\partial \phi} + u \frac{\partial x}{\partial \psi}, \\ 0 &= \frac{\partial \phi}{\partial x} \frac{\partial y}{\partial \phi} + \frac{\partial \psi}{\partial x} \frac{\partial y}{\partial \psi} = u \frac{\partial y}{\partial \phi} - v \frac{\partial y}{\partial \psi}, \\ 1 &= \frac{\partial \phi}{\partial y} \frac{\partial y}{\partial \phi} + \frac{\partial \psi}{\partial y} \frac{\partial y}{\partial \psi} = v \frac{\partial y}{\partial \phi} + u \frac{\partial y}{\partial \psi}. \end{aligned} \quad (3.16)$$

Solving equations (3.16) for the partial derivatives of x and y with respect to ϕ and ψ yields the following,

$$\frac{\partial x}{\partial \phi} = \frac{\partial y}{\partial \psi} = \frac{u}{u^2 + v^2}, \quad (3.17)$$

$$\frac{\partial x}{\partial \psi} = -\frac{\partial y}{\partial \phi} = -\frac{v}{u^2 + v^2}.$$

It follows from equations (3.17) that the Jacobian of the hodograph transformation is

$$\frac{\partial(x,y)}{\partial(\phi,\psi)} = \frac{1}{u^2 + v^2}. \quad (3.18)$$

At large distances from the body the flow must approach a uniform streaming motion and we have

$$\phi = x, \quad \psi = y. \quad (3.19)$$

Define variables \bar{x} and \bar{y} as follows,

$$\bar{x} = x - \phi, \quad \bar{y} = y - \psi. \quad (3.20)$$

Then at large distances from the body ($\phi^2 + \psi^2 \rightarrow \infty$), \bar{x} and \bar{y} vanish.

In view of equations (3.17) and (3.20) we have,

$$\frac{\partial \bar{x}}{\partial \phi} = \frac{\partial \bar{y}}{\partial \psi} = -1 + \frac{u}{u^2 + v^2}, \quad (3.21)$$

$$\frac{\partial \bar{x}}{\partial \psi} = -\frac{\partial \bar{y}}{\partial \phi} = -\frac{v}{u^2 + v^2}.$$

Equations (3.21) are the Cauchy-Riemann conditions and it follows that \bar{x} and \bar{y} are analytic (except at stagnation points $u = v = 0$) and satisfy Laplace's equation

$$\nabla^2 \bar{x} = 0, \quad \nabla^2 \bar{y} = 0, \quad (3.22)$$

where

$$\nabla^2 = \frac{\partial^2}{\partial \phi^2} + \frac{\partial^2}{\partial \psi^2}. \quad (3.23)$$

In terms of the independent variables ϕ and ψ , the outer flow problem is reduced to solving Laplace's equation in the upper half plane $\psi > 0$ with boundary conditions

$$\bar{x}, \bar{y} \rightarrow 0 \quad \text{as} \quad \phi^2 + \psi^2 \rightarrow \infty. \quad (3.24)$$

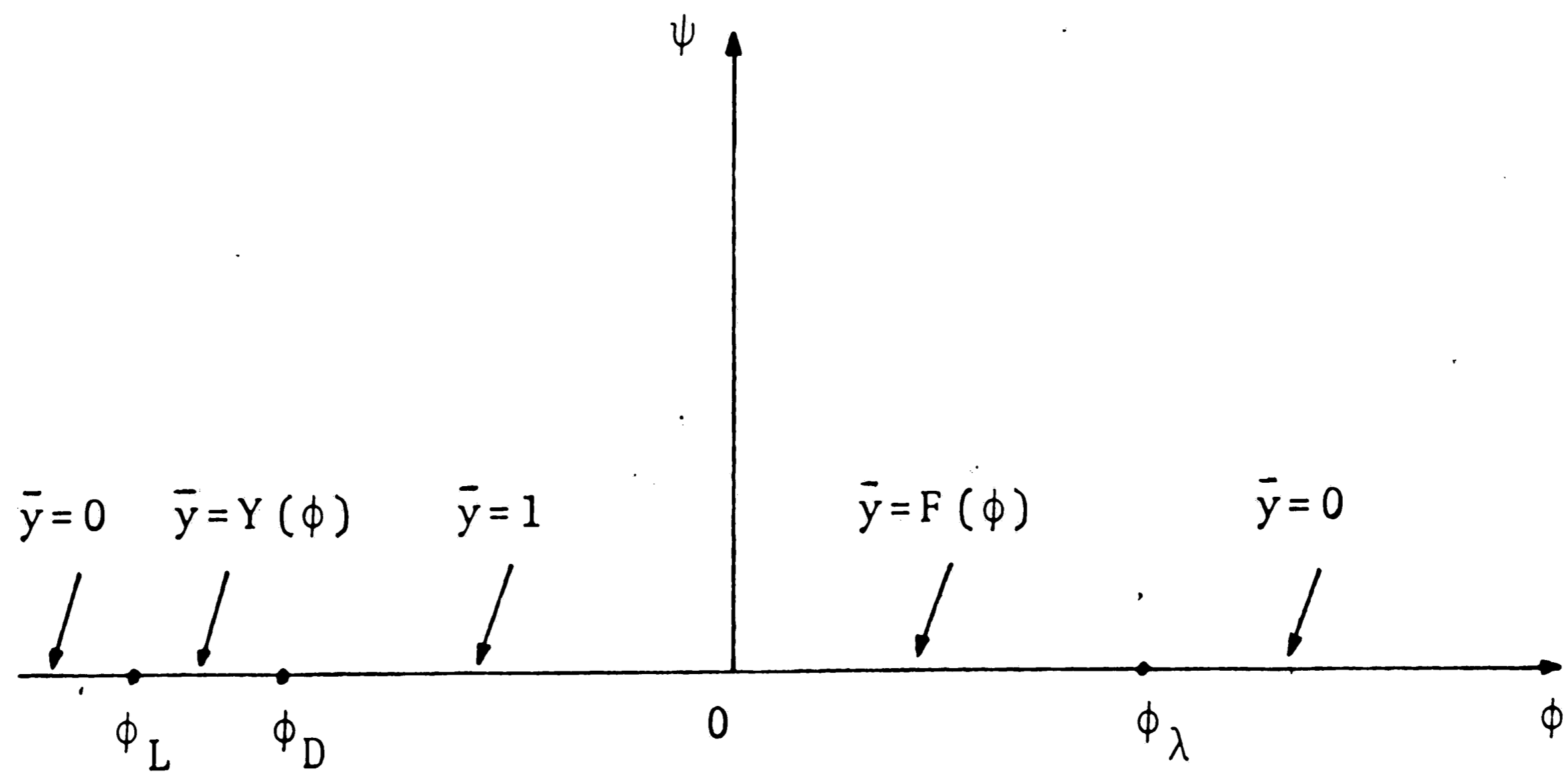
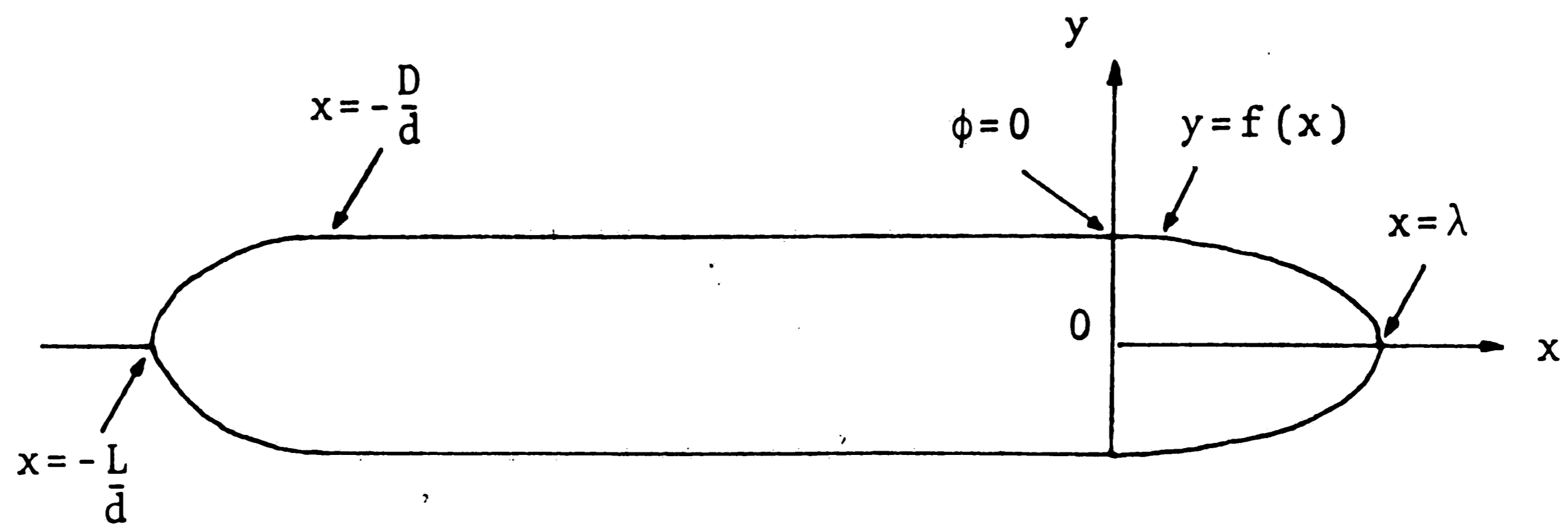


Figure 3.1: Hodograph mapping of (x, y) plane onto (ϕ, ψ) plane.

Along the streamline $\psi = 0$, \bar{y} is given by

$$\bar{y}(\phi, 0) = \begin{cases} 0 & ; \phi < \phi_L \\ Y(\phi) & ; \phi_L \leq \phi \leq \phi_D \\ 1 & ; \phi_D \leq \phi \leq 0 \\ F(\phi) & ; 0 \leq \phi \leq \phi_\lambda \\ 0 & ; \phi > \phi_\lambda \end{cases} \quad (3.25)$$

as illustrated in Figure 3.1, where ϕ_L and ϕ_D are values of the potential at the front stagnation point and the end of the curved leading nose respectively; $Y(\phi)$ is the shape function of the leading nose region; $F(\phi)$ is the function describing the boundary of the separated wake region and ϕ_λ is the potential at the rear stagnation point.

Since \bar{y} satisfies Laplace's equation (3.22), the solution in the upper half plane $\psi > 0$, can be written in terms of the distribution of \bar{y} along $\psi = 0$ as

$$\bar{y}(\phi, \psi) = \frac{1}{\pi} \int_{-\infty}^{\infty} \frac{\psi \bar{y}(s, 0)}{(\phi-s)^2 + \psi^2} ds \quad (3.26)$$

It follows from equation (3.25) that

$$\bar{y}(\phi, \psi) = \frac{\psi}{\pi} \int_{\phi_L}^{\phi_D} \frac{Y(s)}{(\phi-s)^2 + \psi^2} ds + \frac{1}{\pi} \left[\tan^{-1} \left(\frac{\phi - \phi_D}{\psi} \right) - \tan^{-1} \left(\frac{\phi}{\psi} \right) \right] \\ + \frac{\psi}{\pi} \int_0^{\phi_\lambda} \frac{F(s)}{(\phi-s)^2 + \psi^2} ds. \quad (3.27)$$

The first term on the right side of equation (3.27) may be neglected since ϕ_L and ϕ_D are assumed large. By differentiating equation (3.27) with respect to ψ , carrying out an integration by parts and taking the limit $\psi \rightarrow 0$ we obtain

$$\left. \frac{\partial \bar{y}}{\partial \psi} \right|_{\psi=0} = -\frac{1}{\pi(\phi - \phi_D)} + \frac{1}{\pi} \int_0^{\phi_\lambda} \frac{F'(s)}{s - \phi} ds, \quad (3.28)$$

where the integral is interpreted in the Cauchy principal sense.

Note that in accordance with equations (3.13), the conditions on F are

$$F(0) = 1, \quad F(\phi_\lambda) = 0. \quad (3.29)$$

The first term on the right side of equation (3.28) may be neglected

for $0 < \phi < \phi_\lambda$ since it is assumed that $|\phi_D| \gg 1$. Equation (3.28)

then reduces to

$$\left. \frac{\partial \bar{y}}{\partial \phi} \right|_{\psi=0} = \frac{1}{\pi} \int_0^{\phi_\lambda} \frac{F'(s)}{s-\phi} ds. \quad (3.30)$$

In accordance with our model, the shear layer defining the boundary of the wake becomes a dividing streamline in the limit $Re \rightarrow \infty$. It is assumed that there is a jump in the tangential velocity across the dividing streamline. Let u_i and u_o denote the velocities just inside and outside the dividing streamline respectively. Then according to the Bernoulli law, we have

$$\frac{P_i}{\rho} + \frac{1}{2} u_i^2 = c_i$$

and

$$\frac{P_o}{\rho} + \frac{1}{2} u_o^2 = c_o, \quad (3.31)$$

where P_i and P_o are the dynamic pressures inside and outside the wake respectively; ρ is the density of the fluid and c_i and c_o are constants. Since the pressure must be continuous across the dividing streamline, $P_i = P_o$. Hence,

$$u_i^2 - u_o^2 = c_i - c_o, \quad (3.32)$$

from which it follows that

$$u_o = \sqrt{A^* + u_i^2}, \quad (3.33)$$

where A^* is the difference in the Bernoulli constants ($A^* = c_o - c_i$).

In view of equation (3.12),

$$u_o = \sqrt{A^* + \frac{f^2}{\theta^2}}. \quad (3.34)$$

Applying the long eddy approximation along the dividing streamline, we have $v \ll u$ so that equation (3.21) becomes

$$\left. \frac{\partial \bar{y}}{\partial \psi} \right|_{\psi=0} = -1 + \frac{1}{u} \quad (3.35)$$

and it follows from equation (3.34) that

$$\left. \frac{\partial \bar{y}}{\partial \psi} \right|_{\psi=0} = -1 + \frac{\theta}{\sqrt{A + F^2}}, \quad (3.36)$$

where $A = \theta^2 A^*$. Combining equations (3.30) and (3.36), we have

$$-1 + \frac{\theta}{\sqrt{A+F^2}} = \frac{1}{\pi} \int_0^{\phi_\lambda} \frac{F'(s)}{s-\phi} ds. \quad (3.37)$$

This is a nonlinear integro-differential equation in the function $f(\phi)$ which describes the boundary of the separated wake region, with conditions

$$F(0) = 1, \quad F(\phi_\lambda) = 0, \quad F'(0) = 1. \quad (3.38)$$

θ and A are to be specified and ϕ_λ is to be determined.

4. OPEN WAKE SOLUTION

4.1 SOLUTION TECHNIQUE

The integral equation (3.37) with conditions (3.38) may be inverted using the results of Appendix C; Ece, Varley, Walker (1986) to obtain

$$F'(\phi) = -\frac{1}{\pi} \int \frac{\phi}{\phi_\lambda - \phi} \int_0^{\phi_\lambda} \frac{\phi_\lambda^{-s}}{s} \left[-1 + \frac{\theta}{\sqrt{A+F^2(s)}} \right] \frac{ds}{s-\phi}, \quad (4.1)$$

$$0 < \phi < \phi_\lambda.$$

Note that it has been assumed in the inversion that F has a square root singularity at $\phi = \phi_\lambda$. Integrating the first term in (4.1) we have

$$F'(\phi) = - \int \frac{\phi}{\phi_\lambda - \phi} - \frac{\theta}{\pi} \int \frac{\phi}{\phi_\lambda - \phi} \int_0^{\phi_\lambda} \frac{\phi_\lambda^{-s}}{s} \frac{\theta}{\sqrt{A+F^2(s)}} \frac{ds}{s-\phi}. \quad (4.2)$$

Integrating equation (4.2) and applying the boundary condition

$F(0) = 1$ yields

$$\begin{aligned}
F(\phi) = & 1 + \sqrt{\phi(\phi_\lambda - \phi)} - \frac{\phi_\lambda}{2} \arccos\left(\frac{\phi_\lambda - 2\phi}{\phi_\lambda}\right) \\
& + \frac{\theta}{\pi} \int_0^{\phi_\lambda} \left[\sqrt{\frac{\phi_\lambda - s}{s}} \arccos\left(\frac{\phi_\lambda - 2\phi}{\phi_\lambda}\right) \right. \\
& \left. - \log \left| \frac{2\sqrt{s(\phi_\lambda - s)\phi_\lambda(\phi_\lambda - \phi)} + s(\phi_\lambda - \phi) + \phi(\phi_\lambda - s)}{\phi_\lambda(s - \phi)} \right| \right] \frac{ds}{\sqrt{A + F^2(s)}}, \\
& 0 < \phi < \phi_\lambda.
\end{aligned} \tag{4.3}$$

A more convenient form of equation (4.3) may be obtained by introducing new variables

$$\phi = \phi_\lambda \sin^2 \alpha, \quad s = \phi_\lambda \sin^2 \beta, \tag{4.4}$$

with the range of the variable α being $(0, \frac{\pi}{2})$. Substitution in equation (4.3) yields

$$\begin{aligned}
F(\alpha) = & 1 + \frac{\phi_\lambda}{2} (\sin 2\alpha - 2\alpha) \\
& + \frac{\theta\phi_\lambda}{\pi} \int_0^{\pi/2} \left[4a \cos^2 \beta - \sin 2\beta \log \left| \frac{\sin(\alpha + \beta)}{\sin(\alpha - \beta)} \right| \right] \frac{d\beta}{\sqrt{A + F^2(\beta)}}, \\
& 0 < \alpha < \frac{\pi}{2}.
\end{aligned} \tag{4.5}$$

Applying the condition $F(\phi_\lambda) = F(\frac{\pi}{2}) = 0$, we obtain

$$1 - \frac{\pi}{2}\phi_\lambda + 2\theta\phi_\lambda \int_0^{\pi/2} \frac{\cos^2 \beta}{\sqrt{A+F^2(\beta)}} d\beta = 0, \quad (4.6)$$

or

$$2\theta\phi_\lambda \int_0^{\pi/2} \frac{\cos^2 \beta}{\sqrt{A+F^2(\beta)}} d\beta = \frac{\pi}{2}\phi_\lambda - 1. \quad (4.7)$$

Substitution in equation (4.5) yields

$$F(\alpha) = 1 + \frac{\phi_\lambda}{2} \sin 2\alpha - \frac{2\alpha}{\pi} - \frac{\theta\phi_\lambda}{\pi} \int_0^{\pi/2} \sin 2\beta \log \left| \frac{\sin(\alpha+\beta)}{\sin(\alpha-\beta)} \right| \frac{d\beta}{\sqrt{A+F^2(\beta)}}, \quad (4.8)$$

$$0 < \alpha < \frac{\pi}{2}.$$

Equation (4.8) is a nonlinear integral equation for the shape function $F(\phi)$ and it follows from equation (4.6) that the stagnation point ϕ_λ is given by

$$\phi_\lambda = \left[\frac{\pi}{2} - 2\theta \int_0^{\pi/2} \frac{\cos^2 \beta}{\sqrt{A+F^2(\beta)}} d\beta \right]^{-1}. \quad (4.9)$$

4.2 NUMERICAL SCHEME AND PROCEDURE

Initial approximations of ϕ_λ and the distribution of F are determined and equations (4.8) and (4.9) are evaluated iteratively to generate refined values of ϕ_λ and F .

To obtain the initial approximations of ϕ_λ and F , consider the case when the shear layer is very strong. We then have

$$A = \theta^2(c_o - c_i) \gg 1, \quad (4.10)$$

which signifies a large jump in the tangential velocity across the dividing streamline. Neglecting $F^2(\beta)$ with respect to A in equation (4.9), the initial approximation for ϕ_λ is given by

$$\phi_\lambda = 2 \left[\pi \left(1 - \frac{\theta}{\sqrt{A}} \right) \right]^{-1}. \quad (4.11)$$

Neglecting $F^2(\beta)$ with respect to A in equation (4.1) we have

$$F'(\phi) = - \left(1 - \frac{\theta}{\sqrt{A}} \right) \sqrt{\frac{\phi}{\phi_\lambda - \phi}}. \quad (4.12)$$

Integrating (4.12) and applying the condition $F(0) = 1$, yields the initial approximation of $F(\phi)$,

$$F(\phi) = 1 + \left(1 - \frac{\theta}{\sqrt{A}}\right) \left[\sqrt{\phi(\phi_\lambda - \phi)} - \frac{\phi_\lambda}{2} \arccos\left(\frac{\phi_\lambda - 2\phi}{\phi_\lambda}\right) \right], \quad (4.13)$$

or

$$F(a) = 1 + \left(1 - \frac{\theta}{\sqrt{A}}\right) \frac{\phi_\lambda}{2} (\sin 2a - 2a). \quad (4.14)$$

To evaluate the integrals in equations (4.8) and (4.9), the interval $(0, \frac{\pi}{2})$ was subdivided into N equal sub-intervals and the trapezoidal rule was used. Special care must be taken when evaluating the integral in equation (4.8) since the integrand has a weak logarithmic singularity at $\beta = a_i$. Denote this integral by $I(a_i)$.

Then,

$$I(a_i) = \int_0^{\pi/2} \sin 2\beta \log |\sin(a_i + \beta)| G(\beta) d\beta - \int_0^{\pi/2} \sin 2\beta \log |\sin(a_i - \beta)| G(\beta) d\beta, \quad (4.15)$$

where

$$G(\beta) = \frac{1}{\sqrt{A + F^2(\beta)}}. \quad (4.16)$$

Using the trapezoidal rule for all but two sub-intervals around $\beta = a_i$ in the second integral in equation (4.15), we have

$$\begin{aligned}
I(a_i) = & \frac{h}{2} \sum_{j=1}^N \left[\sin 2\beta_j \log |\sin(a_i + \beta_j)| G(\beta_j) \right. \\
& \left. + \sin 2\beta_{j+1} \log |\sin(a_i + \beta_{j+1})| G(\beta_{j+1}) \right] \\
& + \frac{h}{2} \sum_{\substack{j=1 \\ j \neq i, i-1}}^N \left[\sin 2\beta_j \log |\sin(a_i - \beta_j)| G(\beta_j) \right. \\
& \left. + \sin 2\beta_{j+1} \log |\sin(a_i - \beta_{j+1})| G(\beta_{j+1}) \right] \\
& + I^*(a_i), \tag{4.17}
\end{aligned}$$

where $I^*(a_i)$ is the integral over the two sub-intervals on either side of a_i and is given by

$$I^*(a_i) = \int_{a_i - h}^{a_i + h} \sin 2\beta \log |\sin(a_i - \beta)| G(\beta) d\beta, \tag{4.18}$$

where h is the length of a subinterval. Since $(a_i - \beta)$ is small, we approximate $\sin(a_i - \beta)$ by $(a_i - \beta)$ and evaluating the rest of the integrand at $\beta = a_i$, we have

$$I^*(a_i) = \sin 2a_i G(a_i) \int_{a_i - h}^{a_i + h} \log |\sin(a_i - \beta)| d\beta \tag{4.19}$$

Evaluation of the integral in equation (4.19), in the Cauchy principal sense yields

$$I^*(a_i) = 2h(\log h - 1)\sin 2a_i G(a_i). \quad (4.20)$$

To obtain the shape function $f(x)$ in the physical space, we determine x in terms of ϕ . It follows from equations (3.17) and (3.34) that

$$\frac{\partial x}{\partial \phi} = \frac{1}{u} = \frac{\theta}{\sqrt{A+F^2(\phi)}}. \quad (4.21)$$

Integrating equation (4.21) we have

$$x = \int_0^{\phi} \frac{\theta}{\sqrt{A+F^2(\phi)}} d\phi. \quad (4.22)$$

5. RESULTS AND DISCUSSION

In computing ϕ_λ and the distribution of the shape function, the interval $(0, \frac{\pi}{2})$ was divided into a 100 equal subintervals in order to use the trapezoidal rule for the integrations in equations (4.8) and (4.9). Furthermore, the iteration procedure was continued until the difference in values between successive iterates at each mesh point was less than 10^{-4} .

For each value of $\theta = 0.5, 0.7$ and 0.9 , F was computed for a series of values of A , as illustrated in Figures 5.1, 5.4 and 5.7 respectively. It is observed that for a fixed value of θ , the wake length increases as A is decreased. This trend is consistent with equation (4.9). At a certain value of A the iterative scheme failed to converge; for $\theta = 0.5, 0.7$ and 0.9 these values were $0.08, 0.26$ and 0.55 respectively. These results are illustrated in Figures 5.2, 5.5 and 5.8 respectively. Below these values of A , negative values of F occur near the rear stagnation point of the wake. The failure modes for $\theta = 0.5, 0.7$ and 0.9 are illustrated in Figures 5.3, 5.6 and 5.9 respectively. Note that once negative values of F occur it proves impossible to obtain convergence of the numerical scheme. The profiles depicted in Figures 5.3, 5.6 and 5.9 represent intermediate results in a calculation that did not converge.

An important feature observed is that the solution yields short wakes, which is inconsistent with one of the basic model assumptions.

Another interesting trend near the stagnation point is that for a given value of θ , as A is decreased, the slope of $f(x)$ appears to decrease and tend to a finite value.

In conclusion we note that in order to achieve more success, the model assumptions should be changed. Suggestions for a future treatment of this problem are, that the long eddy approximation be relaxed and that the inversion of the integral (3.37) should satisfy the condition that F has zero slope at the stagnation point.

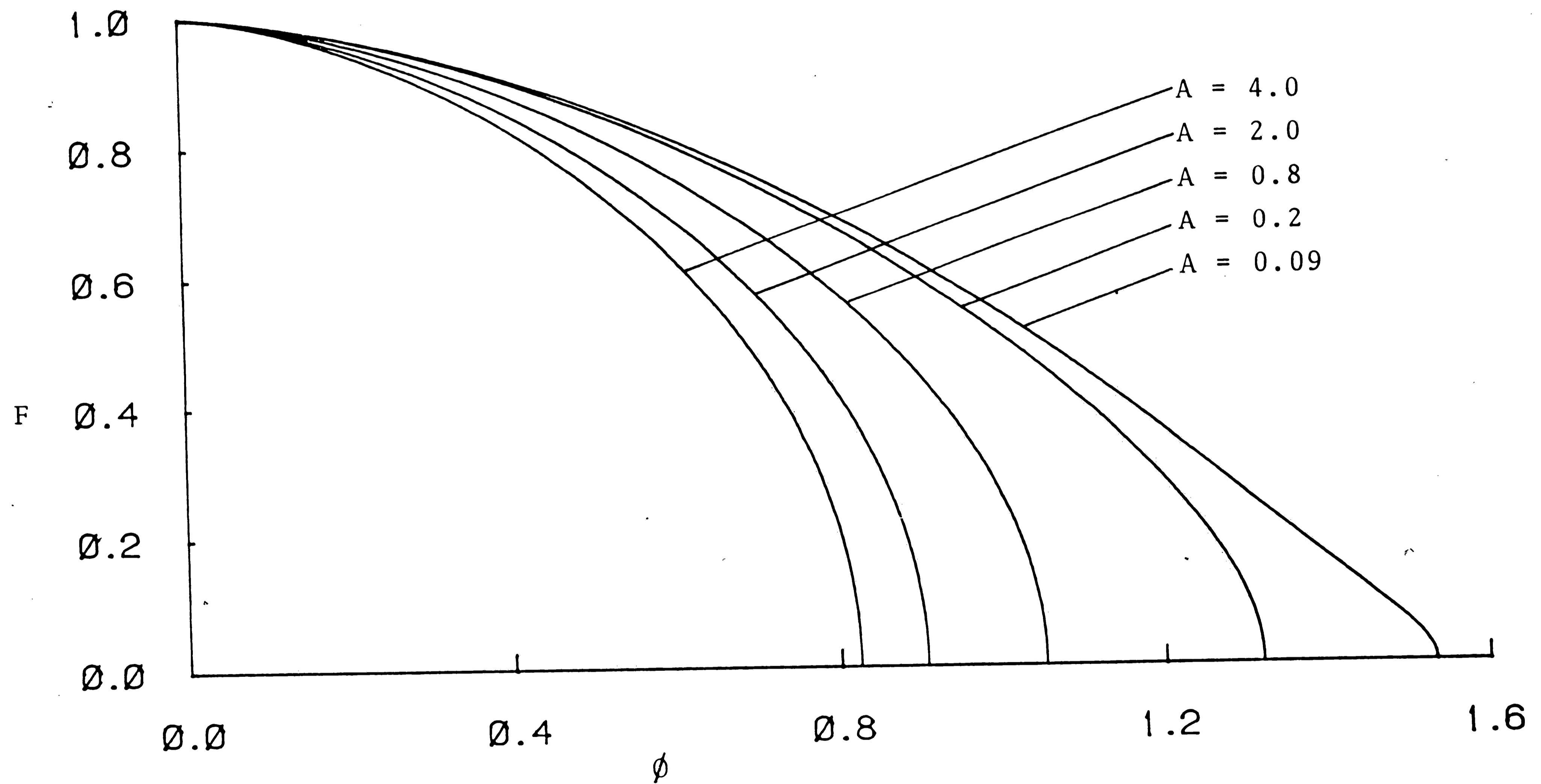


Figure 5.1a: Wake profiles for $\theta = 0.5$.

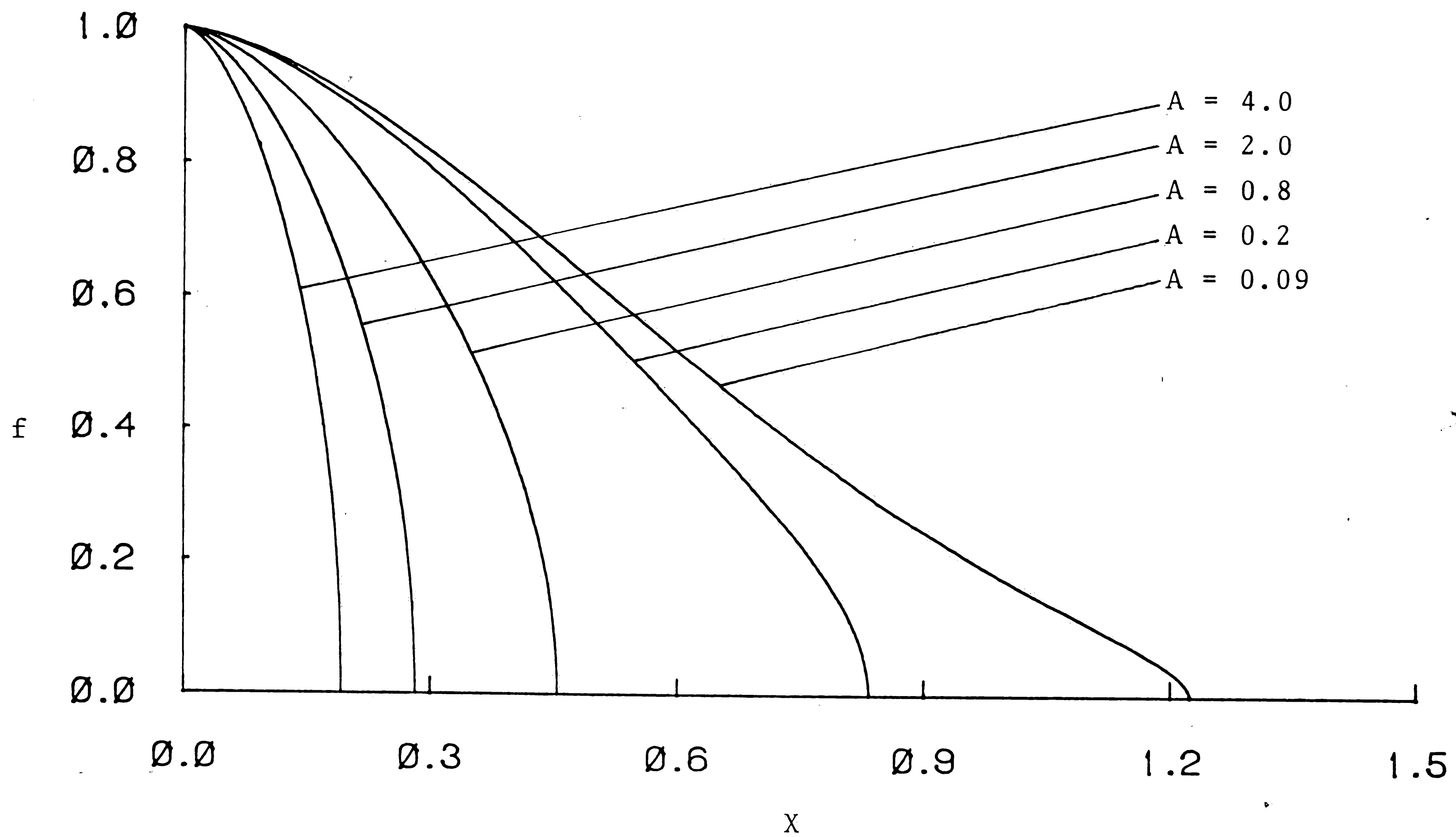


Figure 5.1b: Wake profiles in the physical space for $\theta = 0.5$

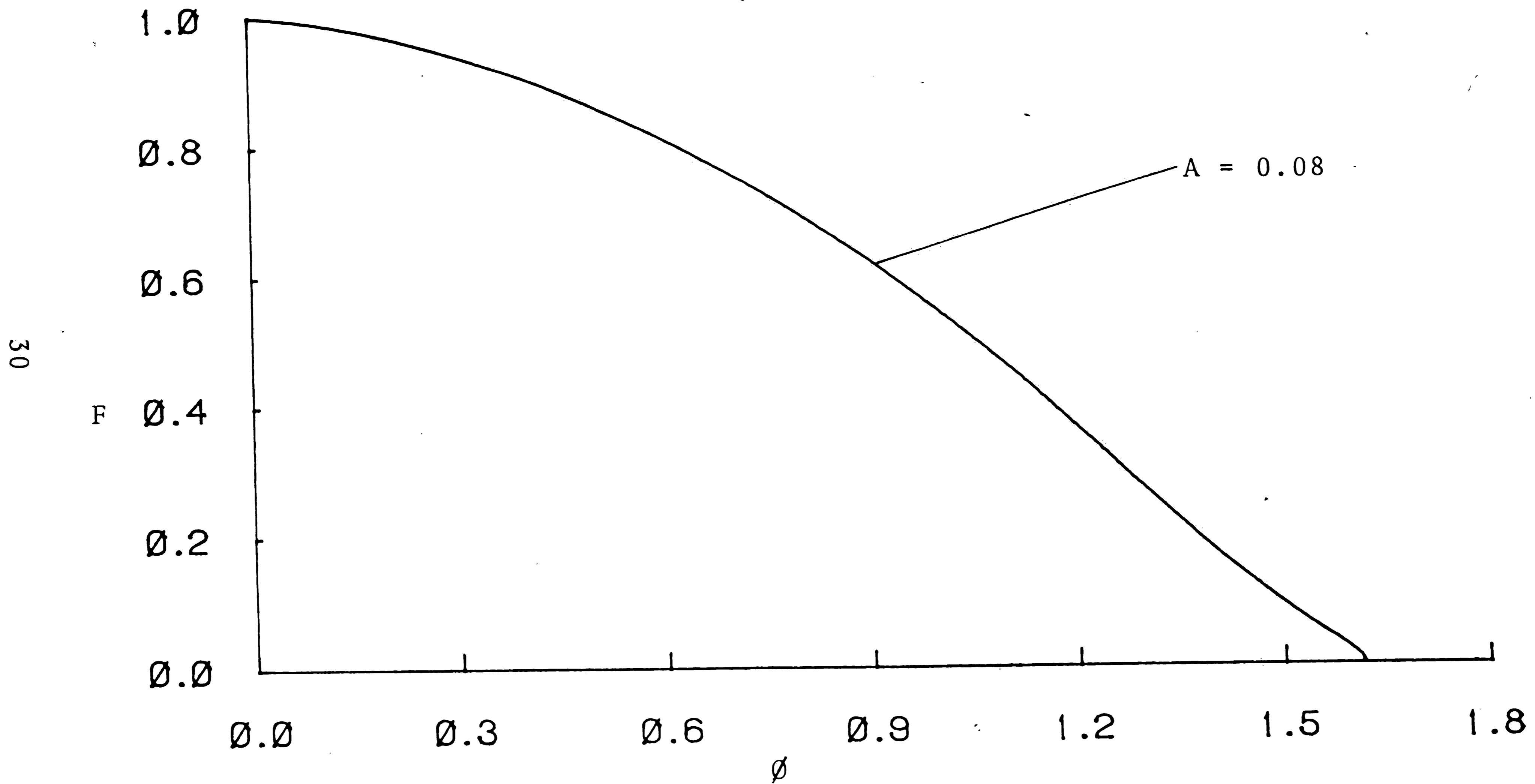


Figure 5.2a: Wake profile for $\theta = 0.5$; Failure

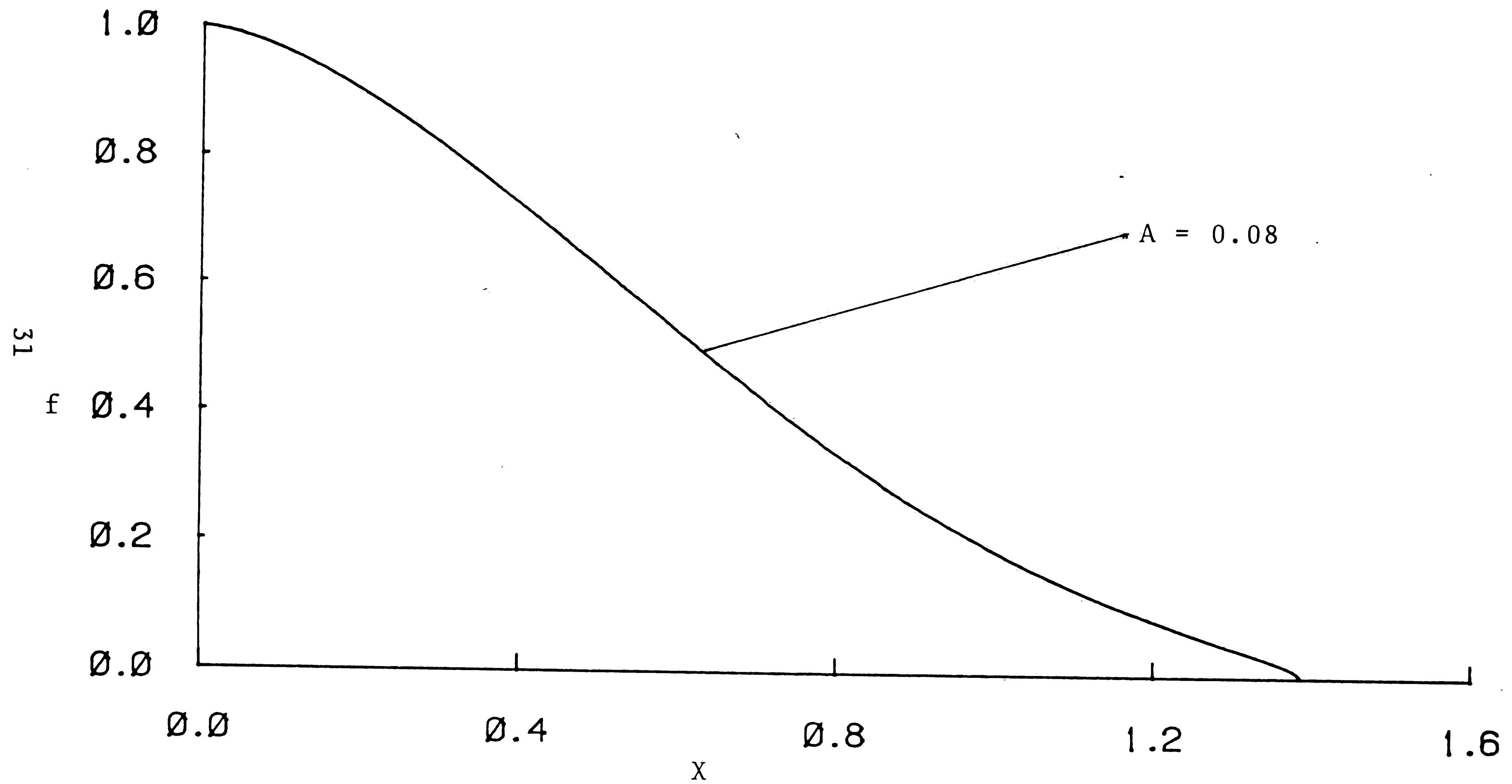


Figure 5.2b: Wake profile in the physical space for $\theta = 0.5$; Failure.

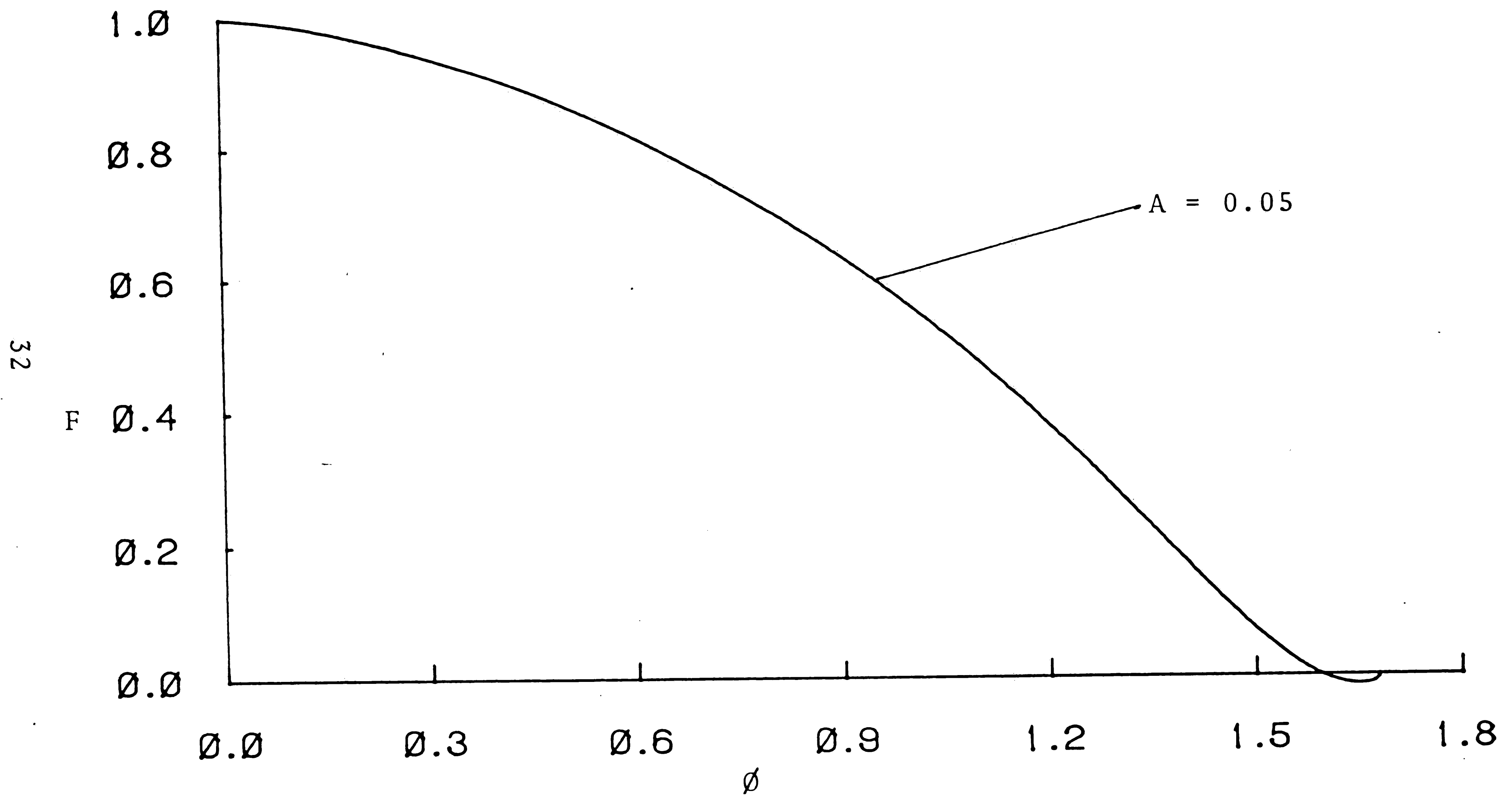


Figure 5.3a: Wake profile for $\theta = 0.5$; Failure mode.

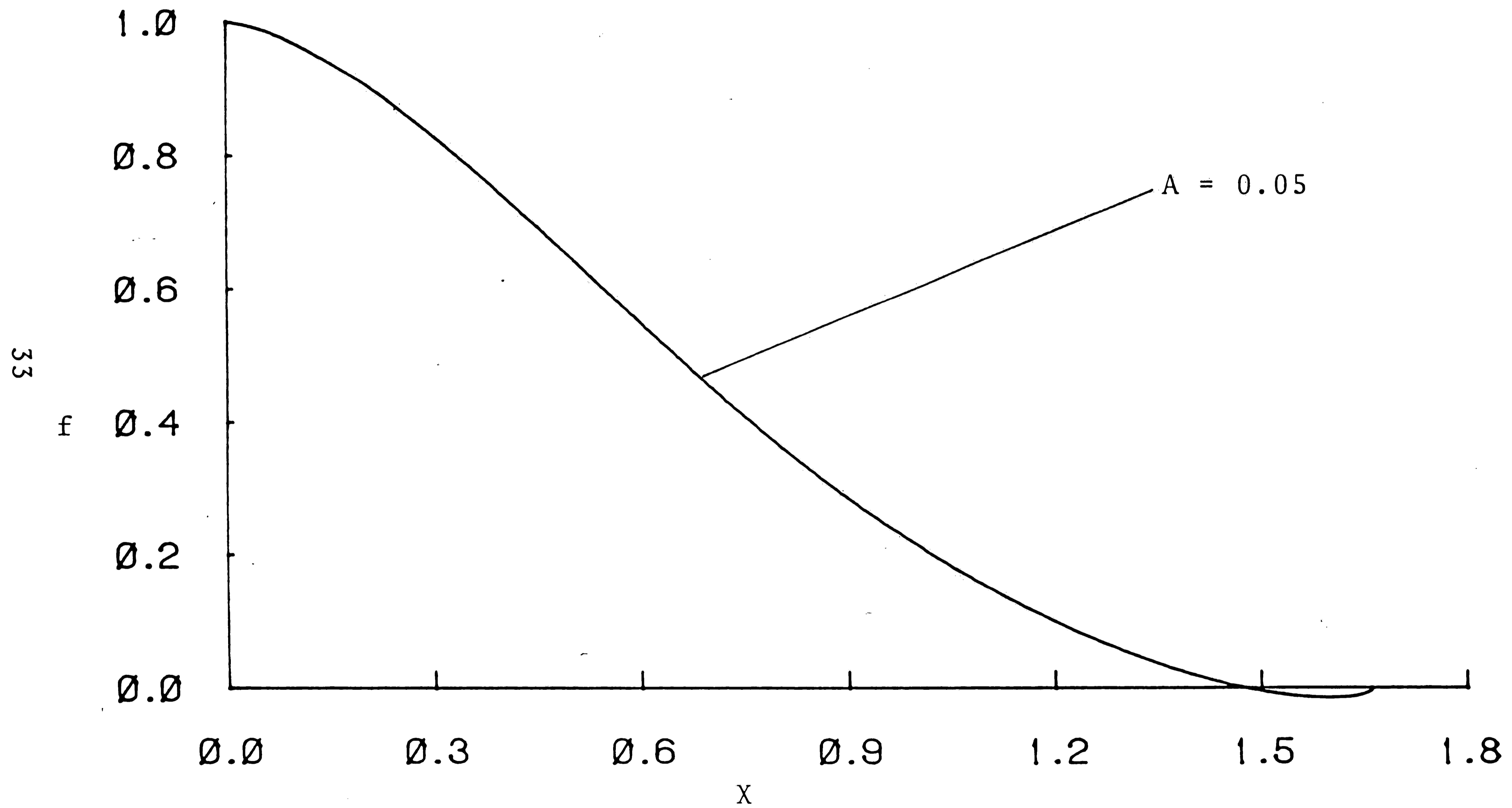


Figure 5.3b: Wake profile in the physical space for $\theta = 0.5$; Failure mode.

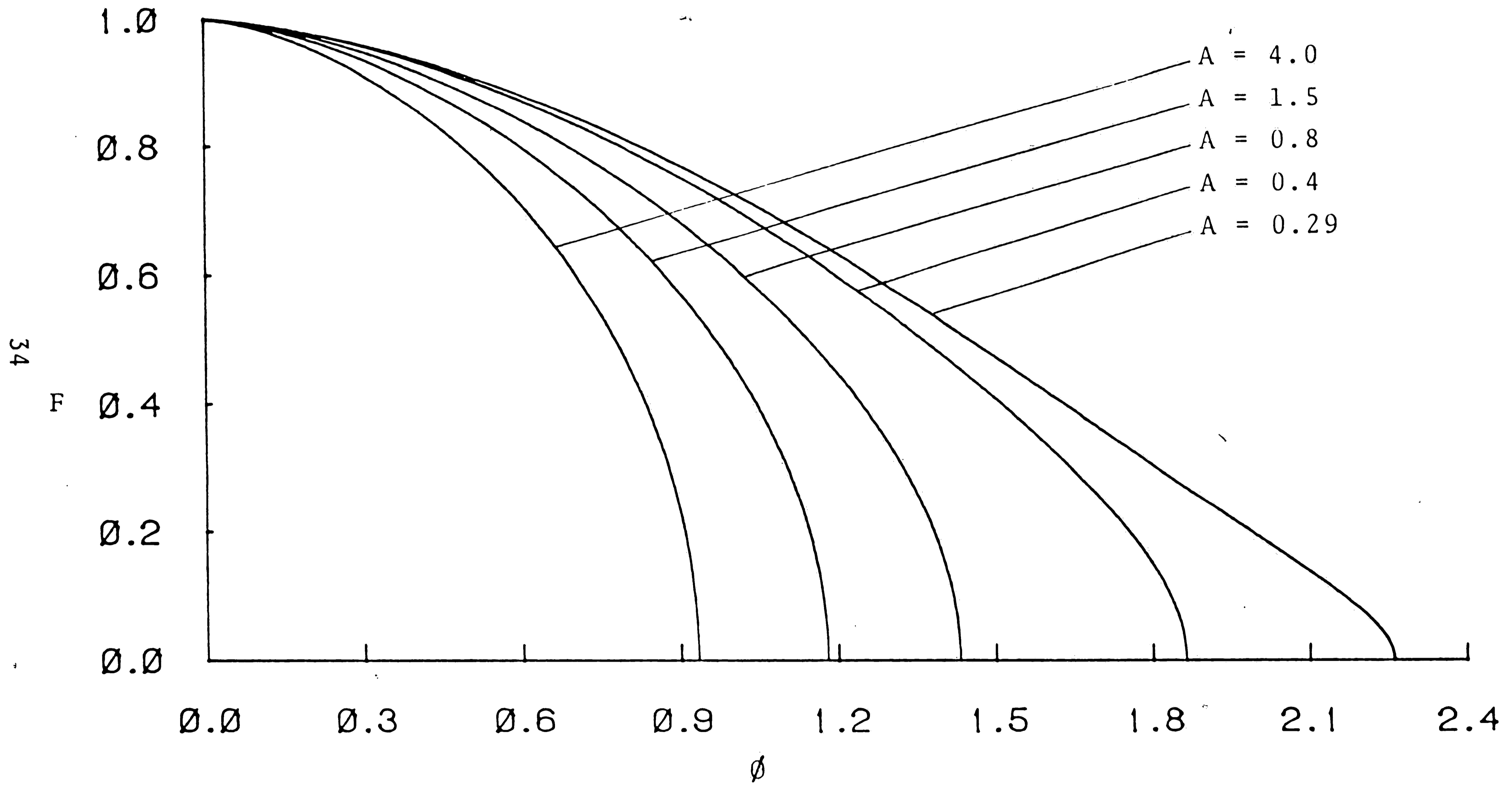


Figure 5.4a: Wake profiles for $\theta = 0.7$.

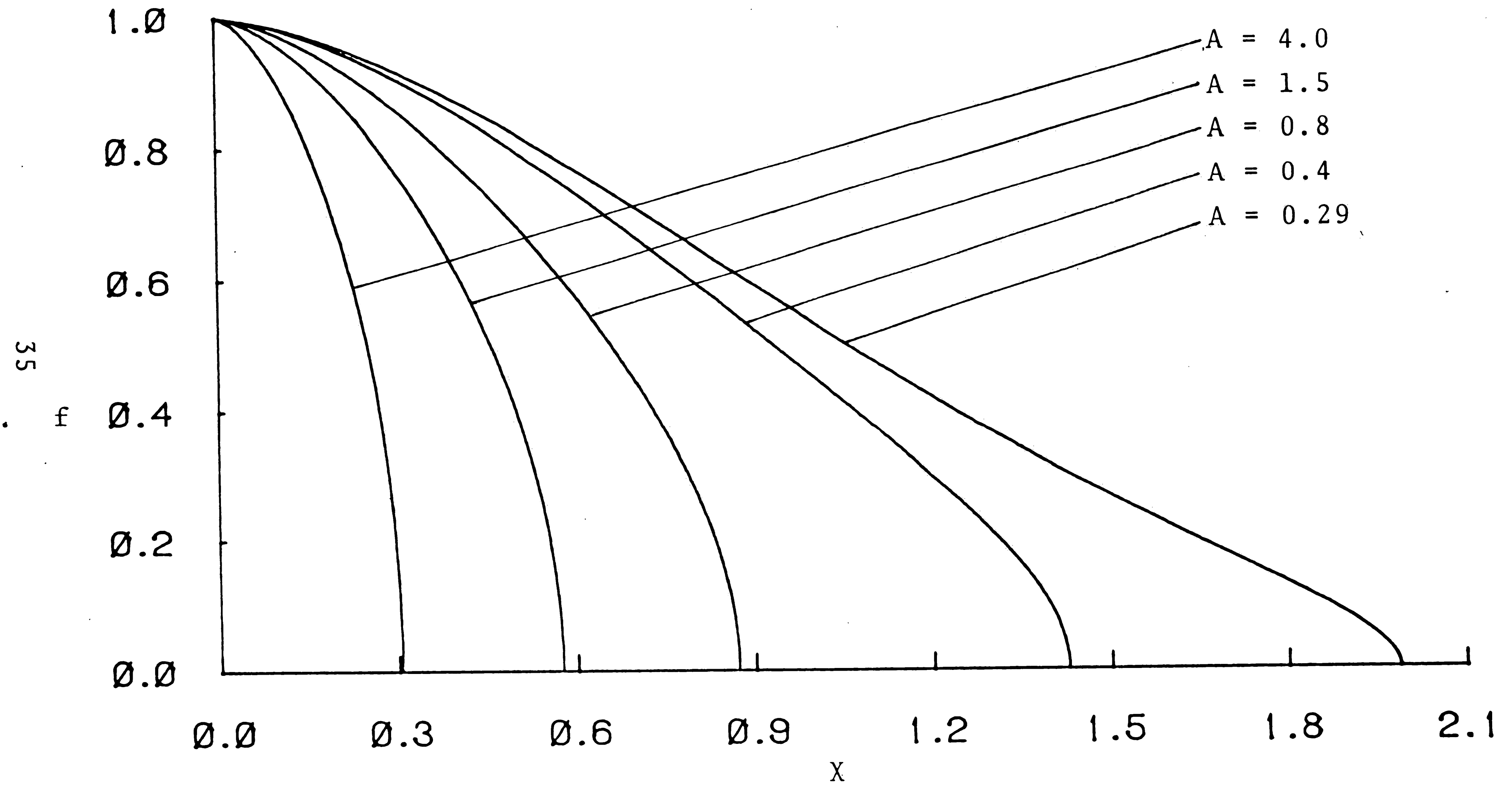


Figure 5.4b: Wake profiles in the physical space for $\theta = 0.7$.

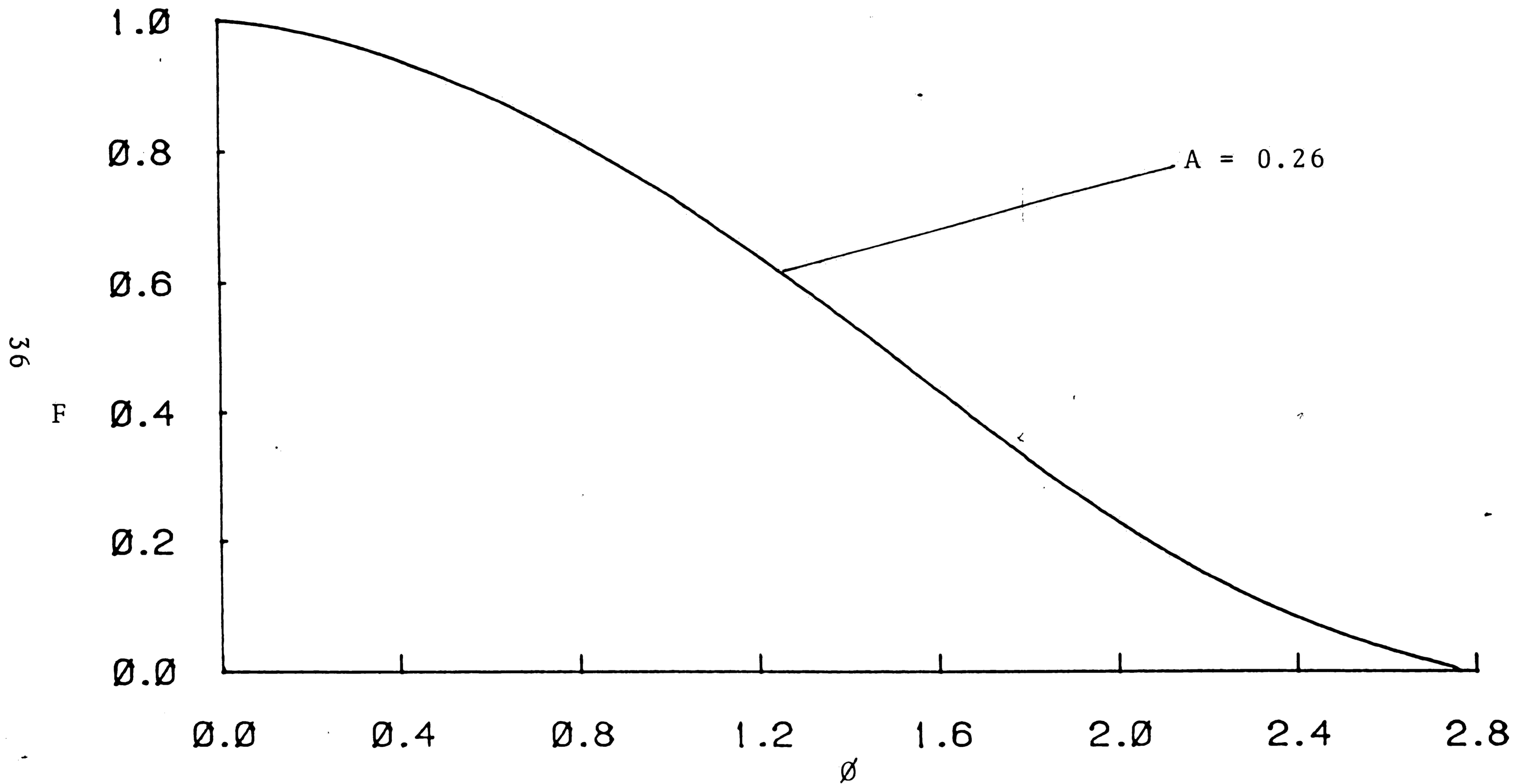


Figure 5.5a: Wake profile for $\theta = 0.7$; Failure.

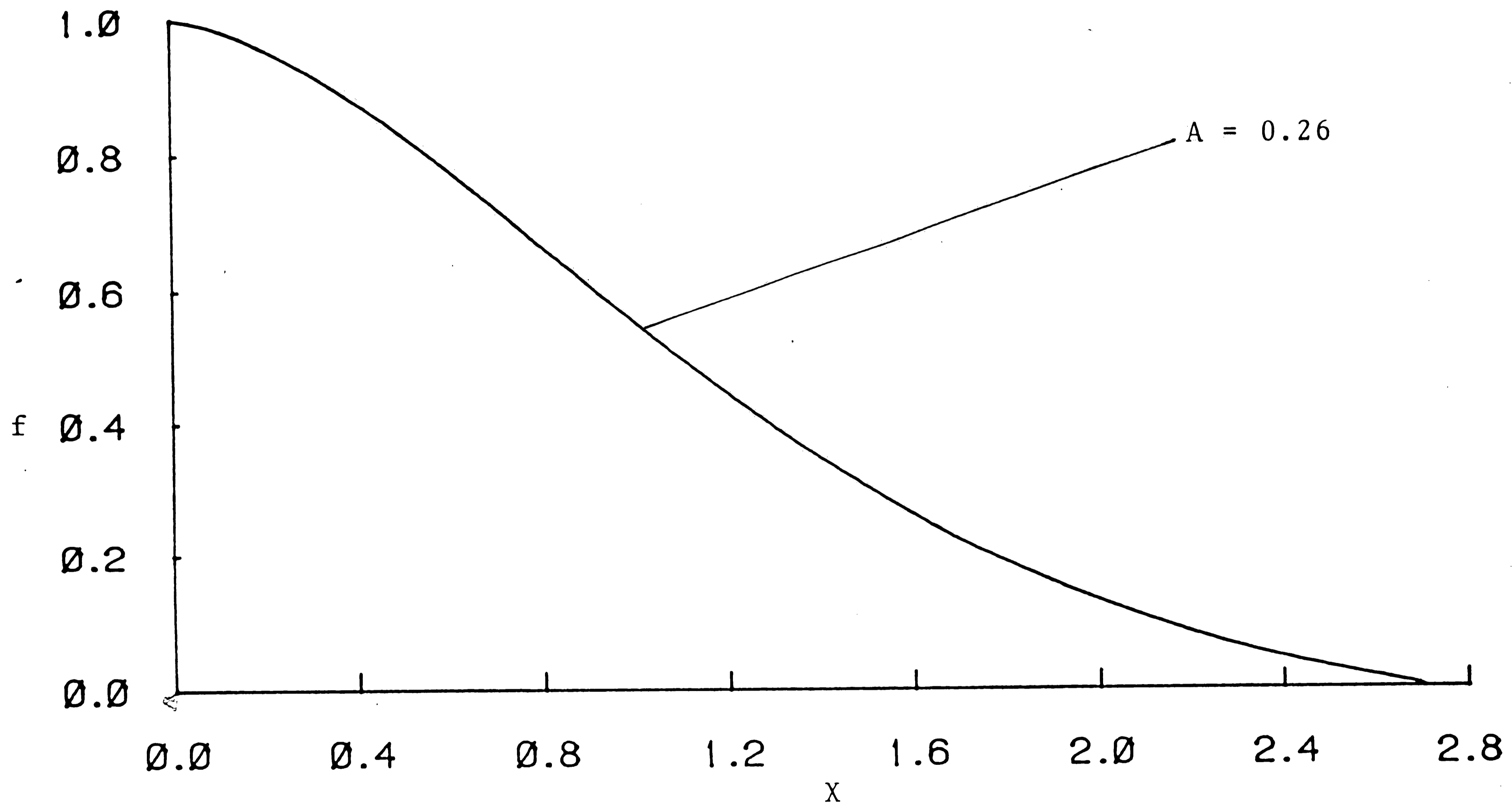


Figure 5.5b: Wake profile in the physical space for $\theta = 0.7$;
Failure.

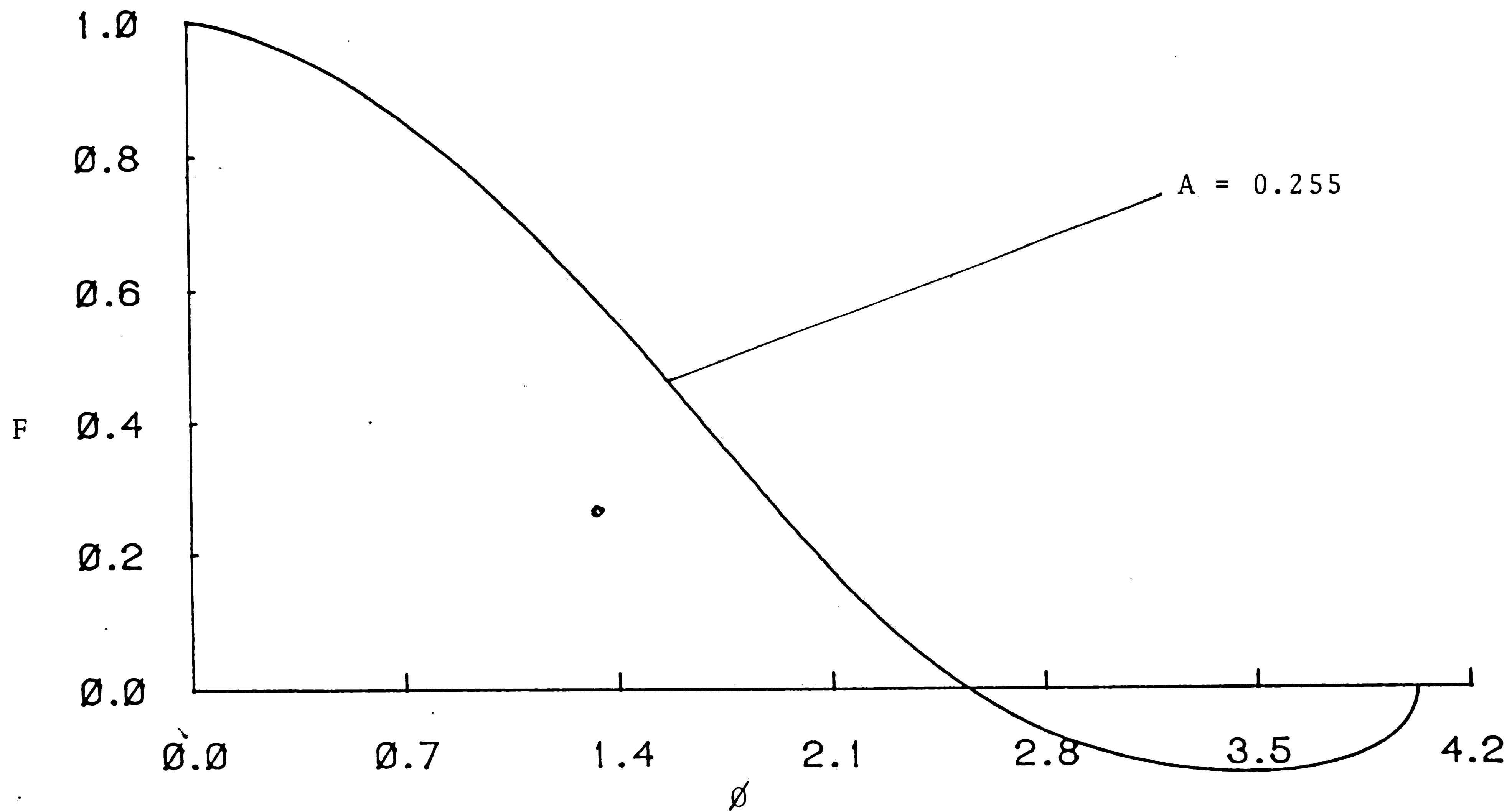


Figure 5.6a: Wake profile for $\theta = 0.7$; Failure mode.

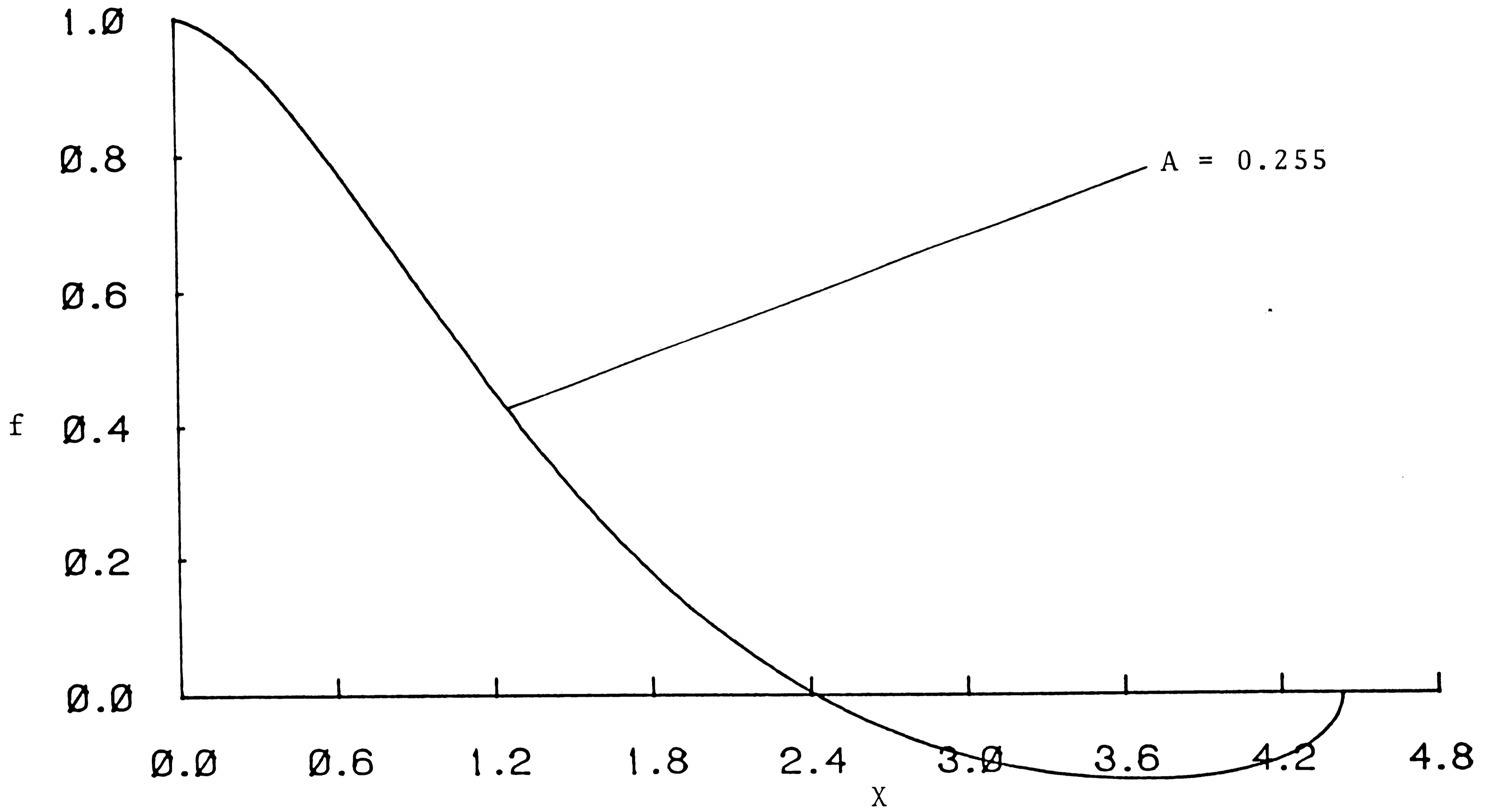


Figure 5.6b: Wake profile in the physical space for $\theta = 0.7$; Failure mode.

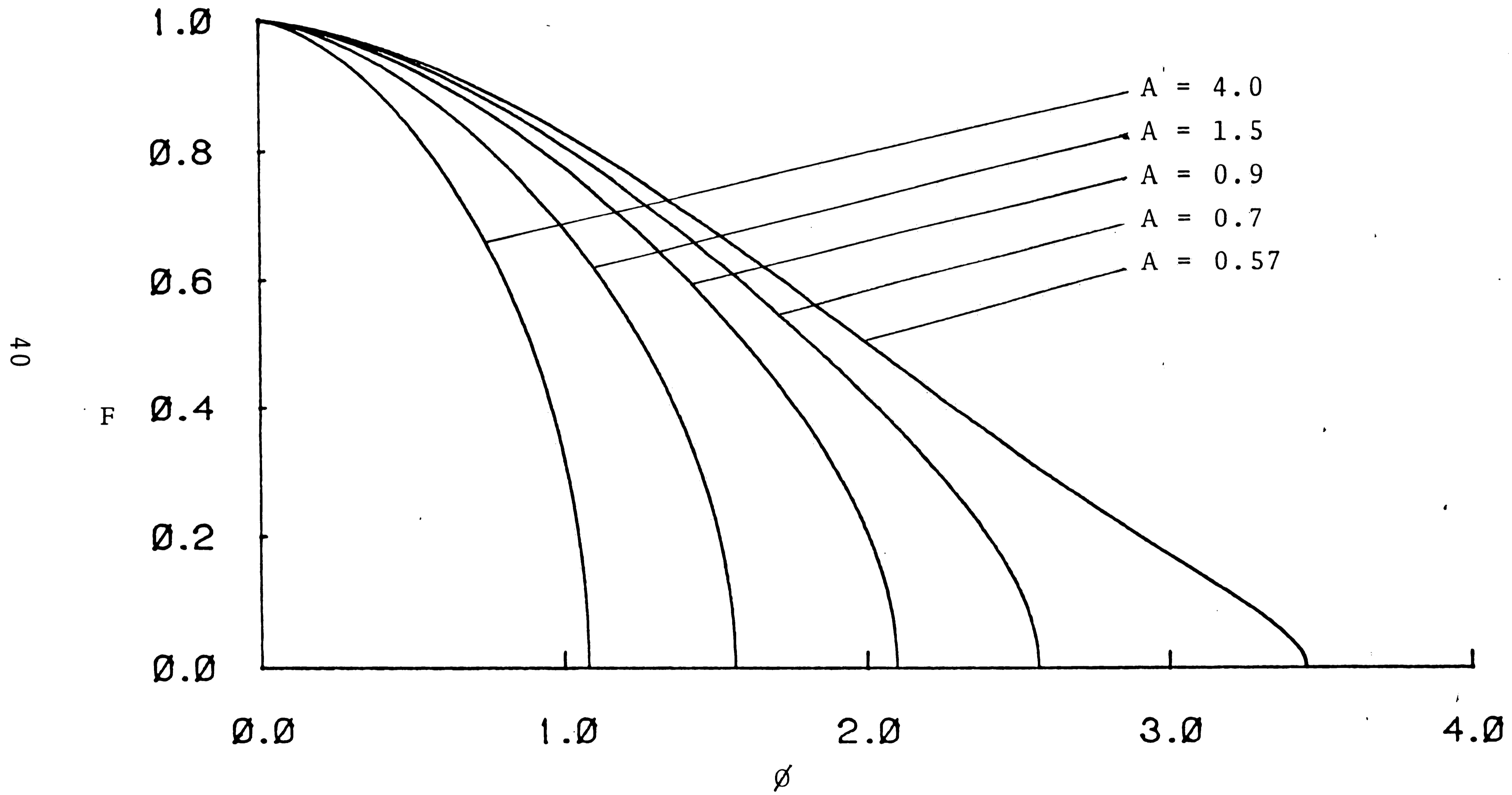


Figure 5.7a: Wake profiles for $\theta = 0.9$.

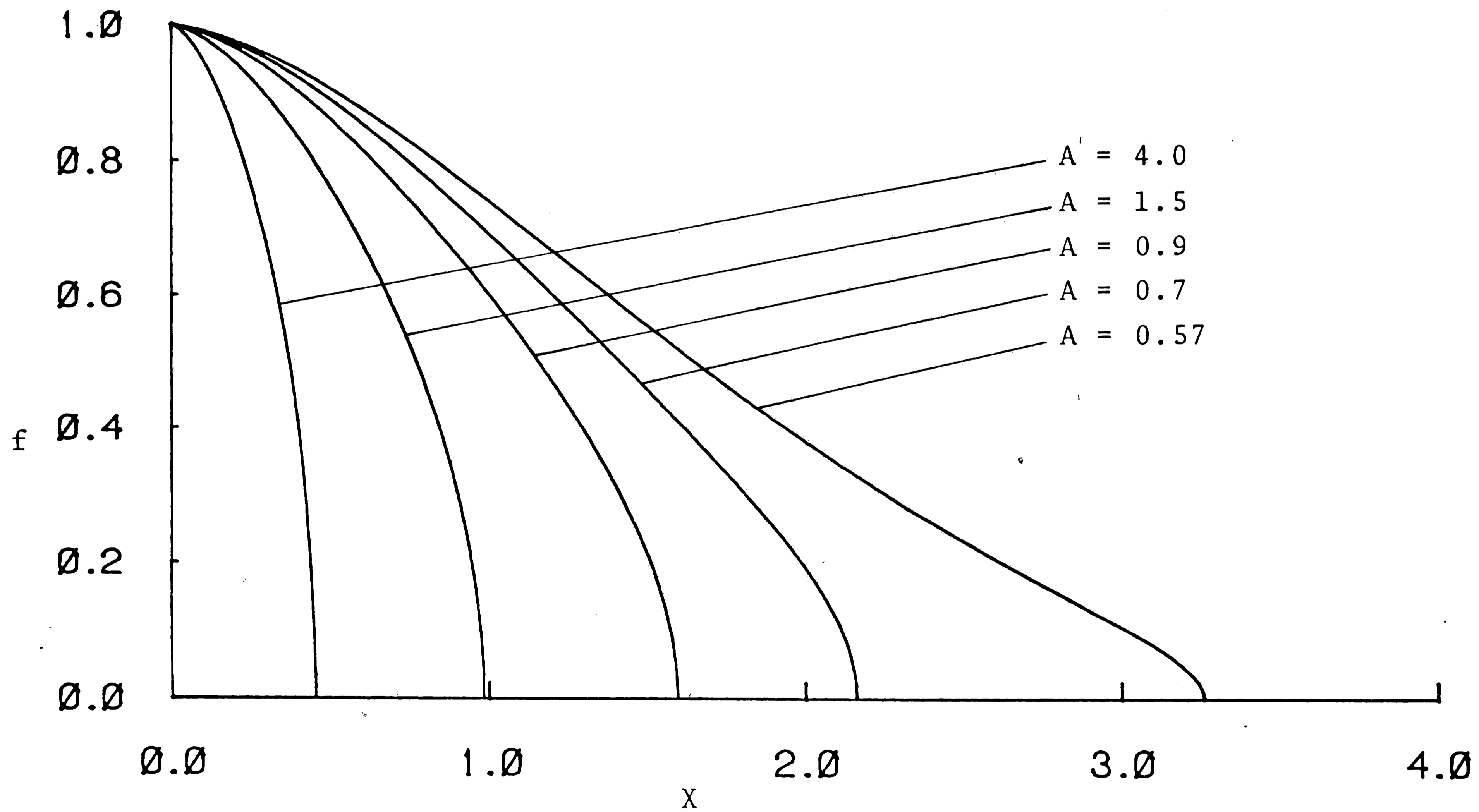


Figure 5.7b: Wake profile in the physical space for $\theta = 0.9$.

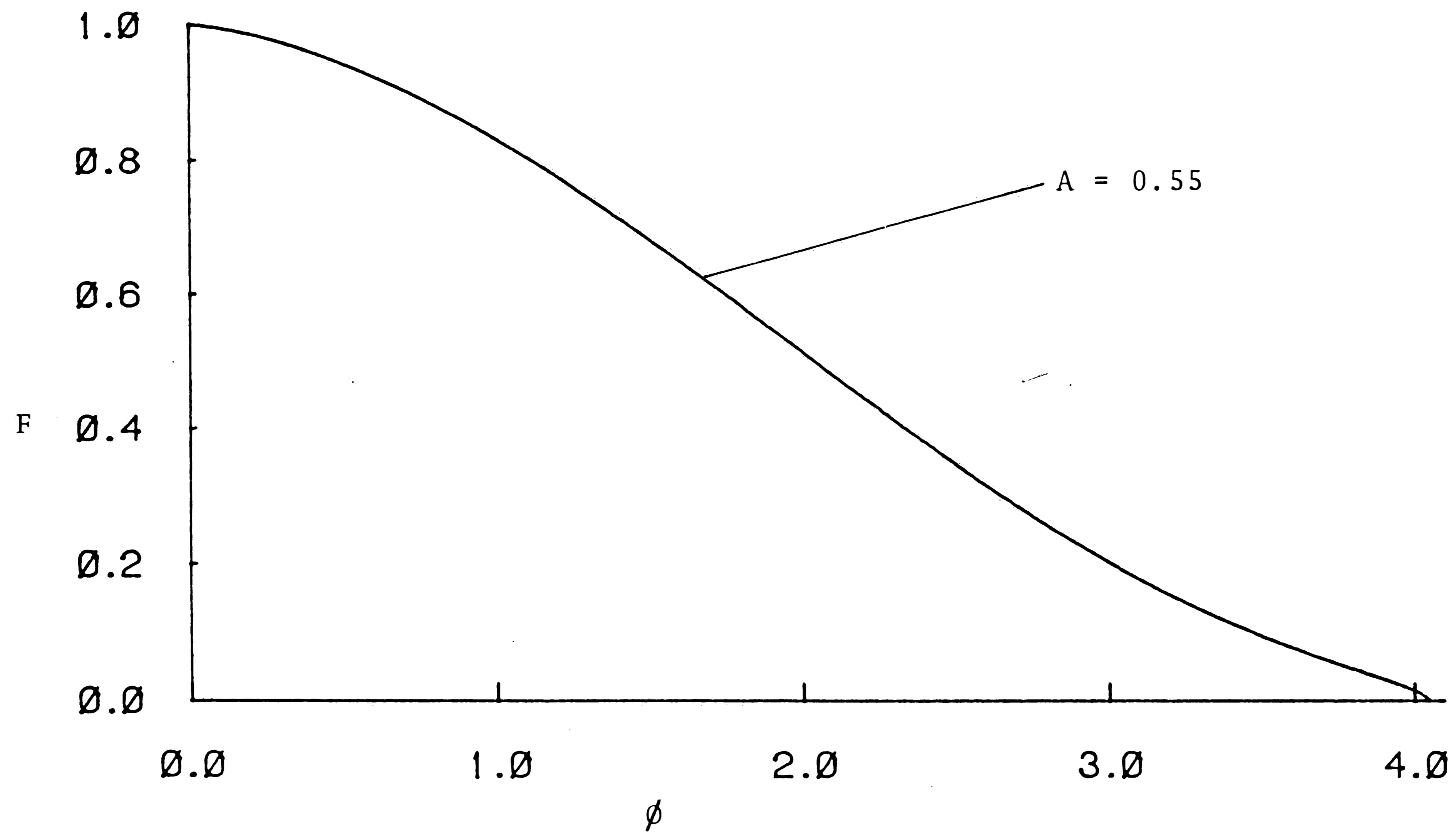


Figure 5.8a: Wake profile for $\theta = 0.9$; Failure.

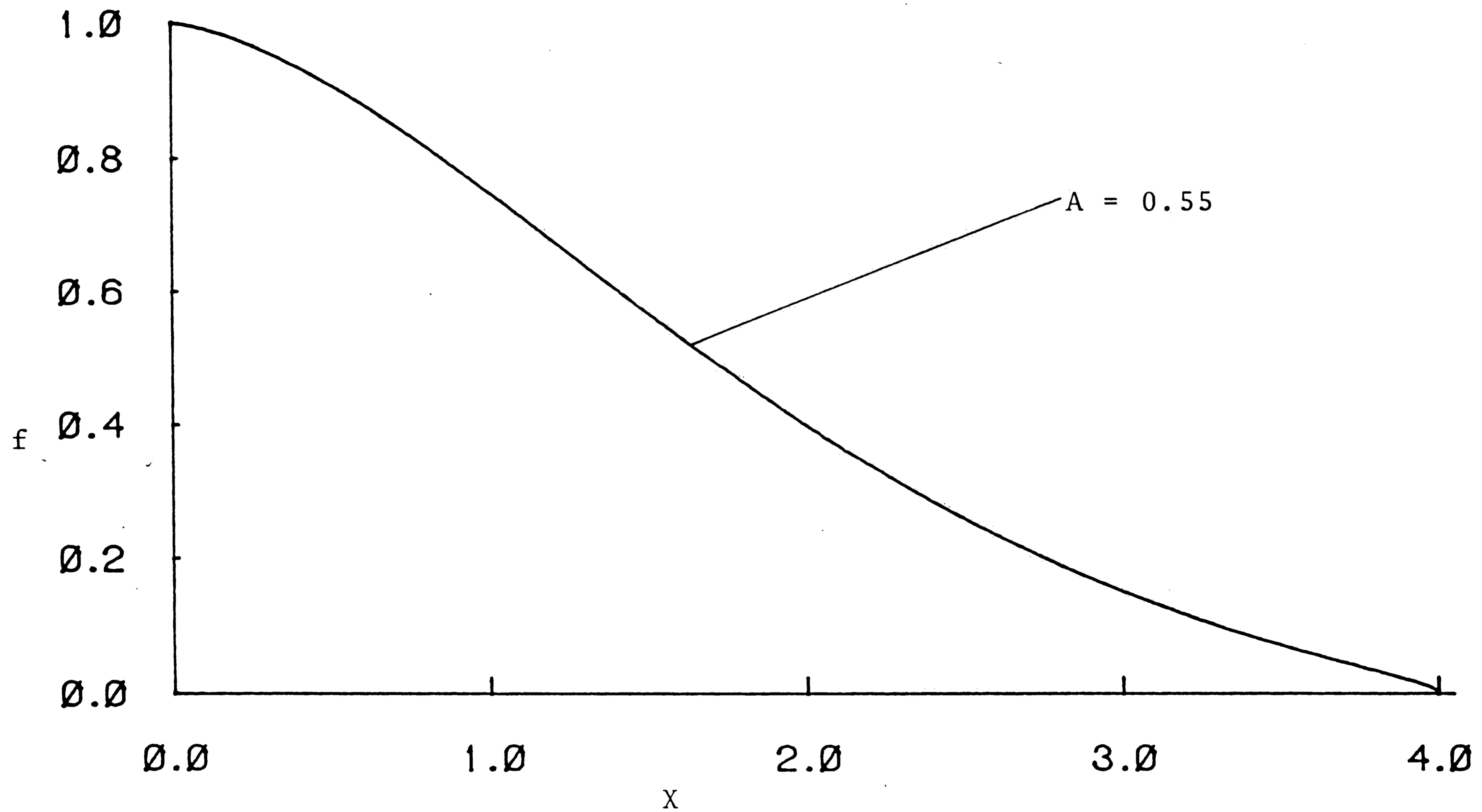


Figure 5.8b: Wake profile in the physical space for $\theta = 0.9$;
Failure.

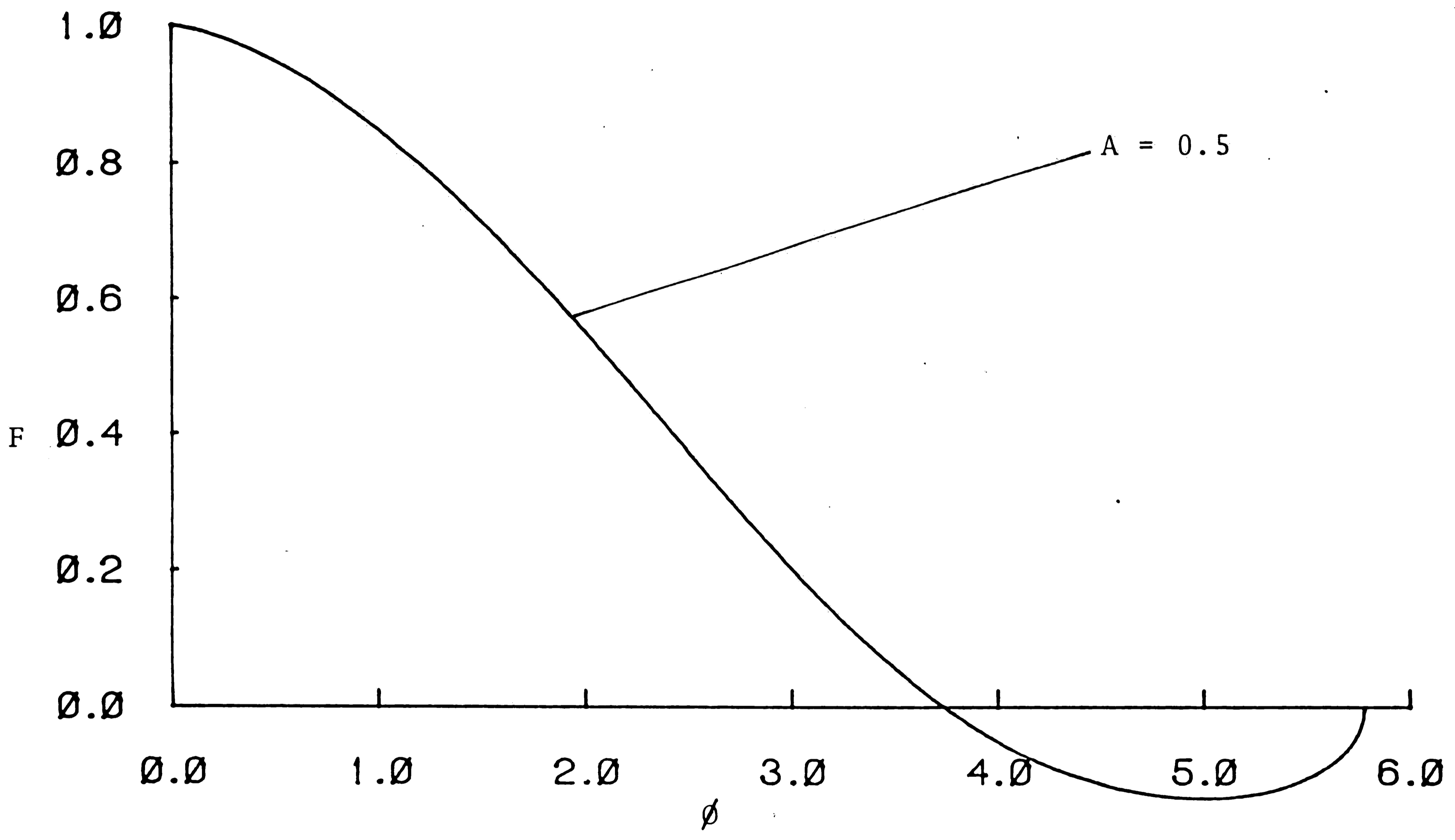


Figure 5.9a: Wake profile for $\theta = 0.9$; Failure mode.

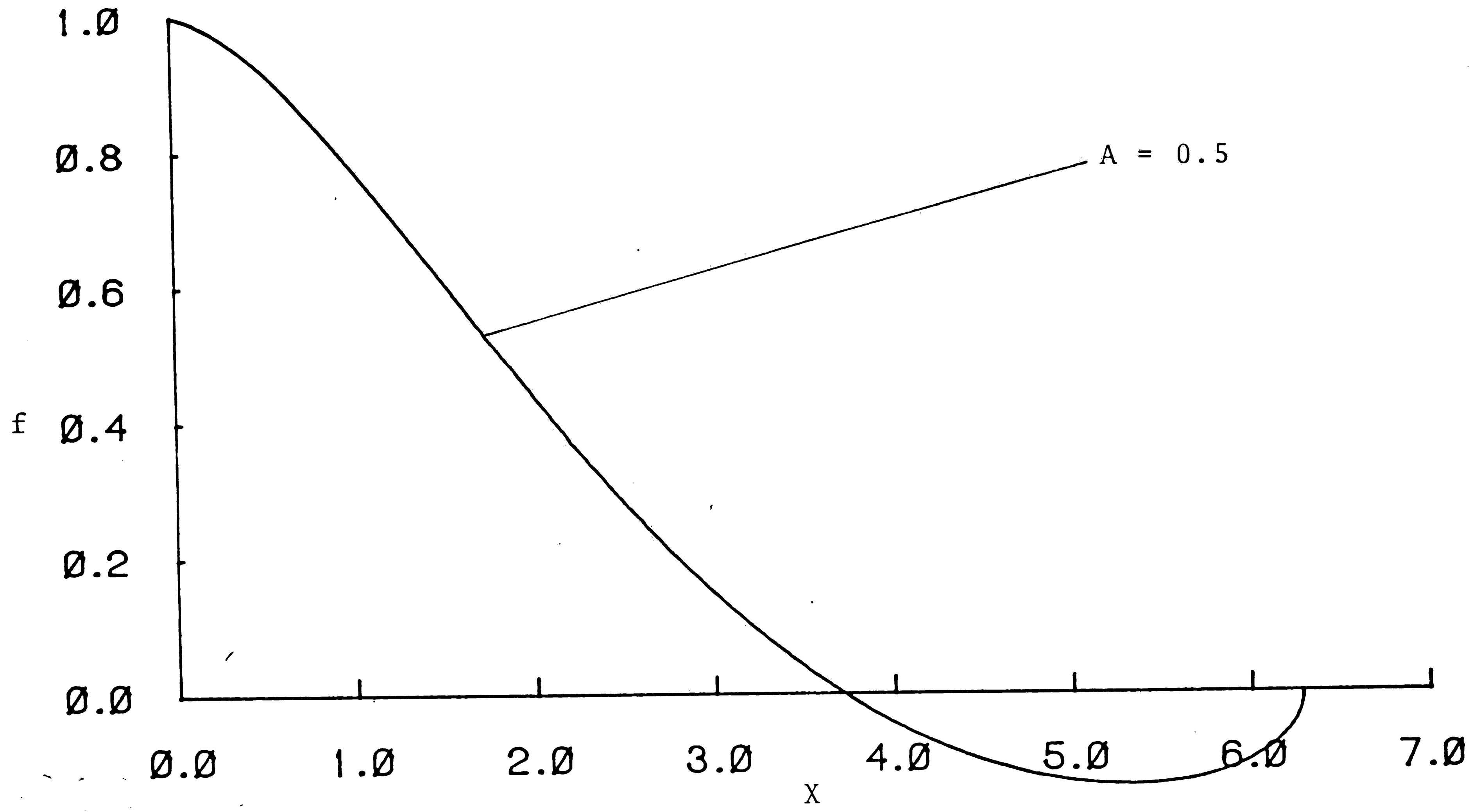


Figure 5.9b: Wake profile in the physical space for $\theta = 0.9$; Failure mode.

LIST OF REFERENCES

1. Batchelor G.K. (1956,a) "On steady laminar flow with closed streamlines at large Reynolds number", J. Fluid Mech. 1:177-190.
2. Batchelor G.K. (1956,b) "A proposal concerning laminar wakes behind bluff bodies at large Reynolds number", J. Fluid Mech. 1:388-398.
3. Batchelor G.K. (1981) An Introduction to Fluid Dynamics, Cambridge University Press, Cambridge.
4. Carrier, G.F., Krook, M. and Pearson, C.E. (1966) Functions of a Complex Variable, McGraw Hill, New York.
5. Ece, M.C., Varley, E. and Walker, J.D.A. (1986) "An analysis of turbulent thermal trailing edge flows", report FM-10, Dept. of Mech. Eng. and Mechanics, Lehigh University, Bethlehem, PA.
6. Haji-Haidari, A. and Smith, C.R. (1984) "A comparative study of the development of the turbulent near wake behind a thick flat plate with both circular and tapered trailing edge geometry", report FM-6, Dept. of Mech. Eng. and Mechanics, Lehigh Univ., Bethlehem, PA.

BIOGRAPHY

Name: Utham Sobrun

Address: Center for the Application of Mathematics
Lehigh University
Bethlehem, PA 18015
U.S.A.

or

P.O. Box 19420
Dormerton, 4015
South Africa

Date and place of birth: Dec. 25, 1954; P.M. Burg, South Africa

Education: Lehigh University, Bethlehem, PA

M.S., Applied Mathematics, May 1987

Thesis: An Analysis of Trailing Edge Flows

University of Durban-Westville, South Africa

B.Sc. Hons., Mathematics, June 1981

Work experience: Lecturer, University of Transkei and University
of Zululand, South Africa

Honors: Institute of International Education Scholarship